Safety in Mines Research Advisory Committee

Final Project Report

A methodology and computer program for applying improved, inelastic ERR for the design of mine layouts on planar reefs

S.M. Spottiswoode and A. M. Milev

Research agency: CSIR: Division of Mining Technology

Project number: GAP 722

Date: August 2002

Reference: 2002 - 0265

Table of Contents

Executive Summary

Use of the mine layout design criteria of ERR (Energy Release Rate), APS (Average Pillar Stress) and ESS (Excess Shear Stress) have not provided a good control of seismicity. It has become apparent that more complex models of rock mass behaviour are needed. Furthermore, such models should be integrated with observed seismicity of recent mining to enable us to better estimate future expected seismicity within a rock mass of uncertain geological structures, strength and virgin stress conditions.

This project follows from GAP612c “The Relationship between ERR and seismic energy release for different geotechnical areas”. It considers concepts of a limit to the load-bearing capabilities of the unmined ground, stress drop during seismic events and the visco-plastic models of Napier and Malan (1997) and Malan (2002). Methodologies and a computer program (MINF) are developed during this project that write synthetic catalogues of seismic events to simulate the rock response to mining. The program MINF was shown here and through a project for Deepmine to be able to provide seismicity catalogues similar to observed seismicity in a number of cases and in several ways.

The program MINF is attached to this document and a model problem can be run directly from this document. Documentation for MINF is provided. Further development and testing will take place for SIMRAC in the next series of project work.

Structure of report.

This report is set up with hyperlinks[1] that can be used to run a sample MINF problem, provide some links between sections and also view a PDF file for a published paper. This short section therefore complements the more lengthy Table of Contents at the start of this report.

Chapter 1 is the Introduction, with motivation and explanation of the steps through which inelastic ERR as a mine layout design tool has moved and is planned to move.

Chapter 2 relates the work done during this project to the planned enabling outputs.

Chapter 3 is a description of rock strength, seismicity generation and time-dependent behaviour as applied in this project and embodied in the MINF program.

Chapter 4 provides a link to the MINF program with a sample demo set-up problem. All files that constitute the final report should reside in the same directory.

Chapter 5 is the user manual for the MINF computer program, with some reference to associated programs.

Chapter 6 is the paper: Milev, A.M. and S.M. Spottiswoode. Effect of the Rock Properties on Mining Induced Seismicity Around the Ventersdorp Contact Reef, Witwatersrand Basin, South Africa, Pure and Applied Geophysics, special issue on induced seismicity, Ed: C Trifu, in Print, 2002. This refereed paper is presented here in PDF format as sent from the publishers.

Chapter 7 is the paper: S.M. Spottiswoode. Aftershocks and foreshocks of mine seismic events. 3rd international workshop on the application of geophysics to rock and soil engineering, GeoEng2000, Melbourne Australia, 2000. An early draft of this paper was submitted as part of the SIMRAC GAP608 final report in March 2000.

Chapter 8 is the paper: S.M.Spottiswoode. Keynote address: Synthetic seismicity mimics observed seismicity in deep tabular mines. 5th Intl Symposium on Rockbursts and Seismicity in mines, S. A. Inst. Min. Metall., pp371-378, 2001. This Symposium was held in South Africa in September 2001.

Lastly, there is a complete reference list for the body of the report as well as the Appendices.

---

[1] Hyperlinking provides the means to navigate within this document itself, if viewed electronically, as well as opening documents. The particular reason, though, for the use of hyperlinks in the report is to provide a direct linkage to running the MINF program with a sample mining problem. Hyperlinked text will be marked in blue and the cursor symbol will change to a hand.

Acknowledgements

Thanks to John Napier for numerous discussions over the last two years. John Napier, John Ryder and Fernando Vieira reviewed drafts of the manuscript.

List of Figures

List of Tables

1 Introduction

1.1 Motivation

At present, 20% or more of the ground in many deep level mines is left behind in the form of pillars or unplanned remnants. These pillars are designed without a rational and mechanistically sound design tool that can be calibrated by using underground observations such as seismicity or stope closure.

It has been shown that, by allowing physically reasonable off-reef deformations (Napier, 1991), ERR including inelastic effects can substantially exceed the conventional, elastic, ERR. Spottiswoode (1997) proposed ideas and methods that can be expanded into routine and improved 3-D modelling for the design of mine layouts.

In a significant advance on previous work, Spottiswoode (1999) generated seismicity in three dimensions for a hypothetical mine geometry, using assumptions of a homogeneous virgin stress field and rock-mass properties. This modelled seismicity showed many of the features observed in mining-induced seismicity:

1. Total seismic moment of the order of the modulus of rigidity multiplied by the volume of elastic deformation: gamma ≈ 1.0.

2. Power law distribution of magnitudes with b ≈ 1.0.

3. Driving stresses ≈ overburden pressure.

4. Qualitatively the “correct” time-dependent behaviour.

5. Locations of seismic events where stresses change, rather than simply on areas with higher ERR.

In summary, it is time that mine layout design methodologies that are based on models of the elastic behaviour of the rock mass, ERR and ESS, are replaced by more realistic models that allow for inelastic deformations and reproduce detailed features of seismicity. Improved capabilities of Personal Computers (PCs) have brought tremendous computing power to every

scientist or engineer. Development of the MINF program described in this report is aimed at extending the elastic criteria towards simulating inelastic effects similar to those observed. Work by Wiles et al (2001) and Lachenicht et al (2001) is also aimed at extending efforts from pure elastic modelling to considering inelastic effects associated with seismicity.

1.2 What is inelastic ERR?

Energy Release Rate (ERR) is defined as the released energy per area mined. In its pure form it was defined for an infinitesimally thin slit within a perfectly linear elastic rock mass. Because it is simple to calculate and provides a minimum estimate of the actual amount of energy released by mining (Napier, 1991), it remains the most widely used means of estimating the potential for seismicity and rockbursting. Mine layouts that are designed to reduce the values of ERR also need to consider other constraints, such as those placed by limitations on the Average Pillar Stress (APS). From mid 1980, several new criteria have been proposed, such as ESS, Volume Excess Shear Stress (VESS) and Rockburst Hazard Index (RHI).

Here is a short and simplified outline of a four-stage progression from the idealised elastic ERR through to a "complete" model for rock-mass deformation. The following section expands on Rock-Mechanics mine layout design criteria.

1.2.1 Stoping within elastic rock mass.

The major shortcoming is that there is no recognition for any inelastic behaviour. Jager and Ryder (1999, p47) provided an elegant discussion on ERR within the purely elastic case. They stated emphatically: "It (ERR) is *not* a direct expression of seismic energy releases due to mining." The proposal by McGarr (1976) that elastic deformations could somehow be accommodated as seismicity in terms of the equivalence of the volume of ride of seismic events with the volume increase of elastic stope closure was ingenious and led to the γ_E parameter that was used in the analysis used by, for example, Milev and Spottiswoode (2002, also included as Chapter 6 of this report).

Jager and Ryder (1999, p47) pointed out that a small "process zone" of damaged material ahead of an advancing face would not significantly affect the calculation of ERR. This simplification is addressed in the next section where this "process zone" is crudely approximated by limiting the on-reef stress.

1.2.2 Limited on-reef stress.

This method provides a very crude allowance for stress reduction on faces and abutments through rock fracturing by capping or limiting the stress on all elements to some value. The major advantage of this approach is the simplicity of implementation within a boundary-element code. Providing a limit to the on-reef stress can be used as a way of combining the ERR and APS criteria within a single tool, as shown by Spottiswoode (1997). Elastic (recoverable) behaviour is retained, although on-reef deformations are non-linear. As with pure elastic ERR, comparisons between modelling and observed seismicity are indirect.

1.2.3 Synthetic seismicity and time dependency from on-reef deformations

A seismic event occurs when a region of rock undergoes a rapid stress and strain change when its strength is exceeded. Interpretation of rock-mass strength is provided in Chapter 5. Most of the work done to date using MINF has been done though implementation of these strength concepts.

1.2.4 Full 4-D simulation of synthetic seismicity and time dependency

The ability to do full 4-D forward modelling is the final target for simulating seismicity and time dependency, but it is not possible with current tools. When we consider all the unknowns and uncertainties of the rock mass and its behaviour, a “full” model that considers every little crack will never be attained. The philosophy of the MINF modelling is to provide increasing capabilities for large-scale mining problems. Extension of MINF from the single-reef or multi-plane modelling towards a better representation of 3-D spatial modelling will be done in stages during 2002/2004 in the SIMRAC project SIM-02-03-01.

1.3 Overview of mine layout design criteria and methodologies

Mine layout designs for control of seismicity and rockburst damage is currently based on the criteria Energy Release Rate (ERR), Average Pillar Stress (APS) and Excess Shear Stress (ESS).

1.3.1 Energy Release Rate.

The original motivation for the use of Energy Release Rate (ERR) involved the analysis of mining of a thin slit within a purely elastic rock mass. Cook et al (1966) stated that when the face is advanced, 50% of the gravitational energy release should appear as seismic energy. Later, Salamon (1993) showed that release of seismic energy in the elastic case was not compulsory.

The major empirical evidence in support of the use of ERR was presented in Figure 1-1 from the 1988 Rockburst and Rockfall Guide (Anon 1988, p85) and consists of a graph based on work done in the early 1980s. This graph shows a clear proportionality between rockbursts per area mined and ERR for mine A and mine B, by using extensive averaging of rockburst rate of many areas with similar values of ERR. Mine A was Western Deep Levels and Mine B was Blyvooruitzicht mine. At the time, stabilizing pillars were not well developed and only a few remnants were being mined in the two mines. Work by Milev and Spottiswoode (2001), attached to this report, has shown that seismicity per volume of elastic closure varies by more than the factor (approximately five) by which the elastic closure is reduced by leaving stabilizing pillars. The evidence in support of ERR as a mine layout design criterion is therefore of a very general nature.

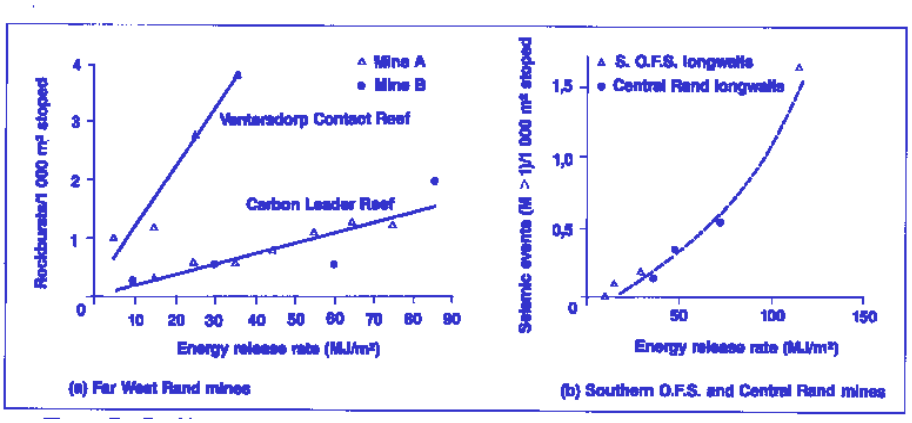

Figure 1-1 Relationship between rockbursts and ERR (from Anon, 1988, p85)

1.3.2 Average Pillar Stress

The size of strike stabilizing pillars has been designed on the basis of a width-to-height ratio more than 10 and Average Pillar Stress (APS) less than 500 MPa. The evidence by Maccelari in Vieira et al (1998) that the amount of back-area seismicity on pillars is independent of pillar width or span indicates that **all** pillars are in the post-failure region and therefore that this APS

criterion is an unreliable measure of stability. Similarly Spottiswoode (1997) suggested that an on-reef limit stress of 250 MPa might be more appropriate than 500 MPa.

1.3.3 Excess Shear Stress, Volume Excess Shear Stress and Rockburst Hazard Index.

The Excess Shear Stress (ESS) criterion was recommended in the 1988 Guide as the best layout design criterion for mining near geological features. Spottiswoode (1990) extended the concept of ESS to estimate failure within the 3-D rock mass. He showed that Volume Excess Shear Stress (VESS) was a more accurate predictor of seismicity than ERR for a large data set from Blyvooruitzicht. VESS has not yet been well proven nor has it been used extensively because it requires special post-processing that is not currently provided by any program. VESS has been included in the Rockburst Hazard Index (RHI) (Esterhuizen, 1997) concept that has been recommended for use in the 1999 Handbook on rockbursts and rockfalls (SIMRAC, 1999). RHI is not used extensively, if at all. Developments by ISS and Mine Modelling Pty Ltd using the computer program MAP3Di (Wiles et al 2001 and Lachenicht et al 2001) and by CSIR Miningtek using the computer program MINF (this report) have overtaken RHI and VESS. It is possible that VESS and RHI will never be widely used for mine design purposes for the following reasons:

- These criteria are totally based on elastic modelling
- They are currently not widely used, if at all.
- User-friendly software is not available.
- Only the author of each criterion has ever acted as a champion for his own criterion.
- A very limited set of back-analyses towards verification has been completed.

Recently, Hofmann et al (2001) have returned to concepts similar to the VESS concept by looking at stress and stress changes on planes parallel to the reef.

The current project has required an approach that moves beyond these criteria towards more realistic rock-mass modelling that allows for explicit inelastic deformation. Two general approaches are possible:

1.3.4 Full 3-D inelastic models

Large-scale mine layout design using models that simulate a very large number of fractures in three dimensions and many time steps is still not practical. Such models have only been developed in a few cases covering small areas and limited time scales. How many of these cases have been followed up? How well have they worked? Very few follow-up studies have indeed been done. There are still major technical issues to be resolved. For example: continuum vs discontinuum, grid-size dependence and heterogeneity of the rock mass. Problems become even more complex when rock fails on three time scales; milliseconds during seismic events, hours during viscous relaxation and days to years during changing mining geometry. It can therefore be said that, in order to consider the complex role of time in rock deformations around mines, a simulation program must be 4-dimensional in nature.

This inherent complexity system must be simplified to keep it amenable for solutions of complex problems. As the standard ERR criterion is a gross oversimplification, we must search for an extended ERR that makes some allowance for inelastic behaviour.

1.3.5 Integration of seismicity and modelling.

Spottiswoode (1999) developed concepts of synthetic seismicity. These concepts have been extended as the main topic of SIMRAC GAP722 as presented in this report.

2 Statement of Output and Progress

This chapter relates the work done during this project to the enabling outputs. It is based on the quarterly reports presented during this study.

2.1 EO1: Expanded studies of modelled seismicity using actual mining layouts. Comparisons with observed seismicity and stope closure profiles in different mining situations.

Regarding development of the MINF code, methodologies were formulated and data sets selected for hypothetical mining layouts and for different mining scenarios. Methods have been developed as extensions to a multi-layer model that was partly developed by Spottiswoode (1999). Comparisons were made between observed and synthetic seismic catalogues in terms of the distribution of seismic events in space and time.

Use of a simple model of viscous relaxation of failed rock results in time-of-day distributions similar to those observed for mining-induced seismicity. A major result is that this behaviour appears to mimic Omori's law of earthquake aftershocks more closely than an exponential decay ($e^{-\lambda t}$) (Chapter 7 from Spottiswoode, 2000). Perhaps this is a reflection of the same power-law behaviour that results in Gutenberg-Richter frequency-magnitude distributions commonly observed.

Comparisons between modelled and observed seismicity in any region and time interval can be carried out in many different ways. At this stage, we define five main categories.

1. **Total action**. This can be measured in different ways, usually by summing event parameters that are some measure of the "strength" or "magnitude" of each event. Summations are often presented over time. Examples of "strength" are the number of events (N) greater than M_{MIN} and summations of seismic moment (ΣM_0), energy (ΣE), apparent volume (ΣV_a) and the hazard estimate (ΣN_F, where $N_F = 10^{M-4.25}$). All of these event parameters can be expressed as $M_0^{\alpha} \times \sigma^{\beta}$, where $\alpha >= 0$ and σ = seismic stress, as listed next.

2. Some measure of seismic **stress.** Apparent, static or dynamic stress may be used.

3. The **magnitude-frequency distribution**. Seismic moment is arguably the most robust parameter that can be estimated from modelling and is generally favoured by seismologists as the best measure of event Magnitude, M. The moment-Magnitude, M(Mo), is therefore probably the best measure of magnitude to use.

4. **Spatial distributions** of seismicity. This can be represented by symbols in three dimensions, as various forms of clustering or inter-event spacing or even contoured. Observed data suffers from location accuracy. Furthermore, the low incidence and the finite source sizes of the largest events cause difficulties with contouring that are still not well controlled.

5. **Time distribution**. As not all the seismicity occurs at blasting time, the distribution of seismicity or strain with the time after blasts is of primary importance. Aftershocks of large events should also be modelled. Figure 2-1 shows the time-dependent decay of seismicity following an increment in face advance in a hypothetical 3-D mining geometry. The seismicity rate followed a logarithmic curve, in agreement with logarithmic creep and Omori's law of aftershocks. The time-dependent behaviour of seismicity following large events and blasts was described by Spottiswoode (2000) and repeated here in Chapter 7.

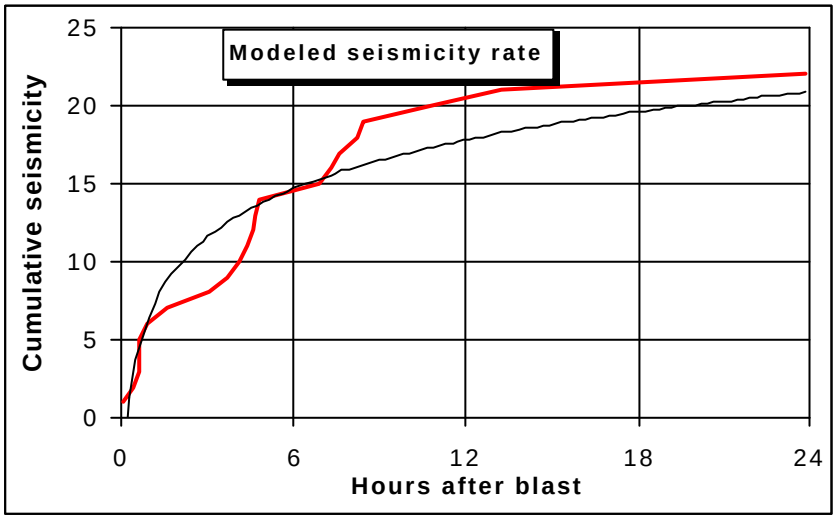

Figure 2-1. Modelled cumulative seismic event rate after face advance with a logarithmic best-fit curve for comparison.

2.2 EO2: Investigate the feasibility of locally improving the spatial resolution of modelling around faces and abutments.

Improved spatial resolution beyond that achieved by the normal 64 by 64 MINSIM patterns is provided in three ways.

1. **Zooming**.

The gridding can be done in more detail through a zoom function by means of which each element is increased from 1X1 to 2X2, 4X4 or 8X8. This results in increased resolutions of 128X128, 256X256 or 512X512. When zooming, MINF takes advantage of the percentage-mined option provided by the MinSim gridding software. Expansion of percentage-mined elements during zooming to 4, 9 or 16 elements takes place through consideration of the local face direction.

2. **Minor steps**.

Face positions are often available only on monthly, three-monthly or even an annual basis. This converts to face advances between successive mining steps of about 5m to 180m. This would amount, in the worst case, to up to 36 grid blocks at a block size of 5m. MINF allows for the face position to be advanced by only one grid block at a time using several different growth rules. This allows for use of face positions that have been digitised with a face advance more than the final grid size after zooming. The MINSIM patterns are defined as describing "**major steps"** and the small face advance as "**minor steps"**.

3. **Zonking**.

The stresses on elements can be reduced gradually so as not to transfer stresses on to neighbouring elements too rapidly. The term "zonk" was coined by ITASCA® to describe a process of gradual, step-wise stress reduction while mining elements in the FLAC™ program. This process can simulate the effect of a face advance of one metre even when the grid size is many metres.

These refinements to spatial resolution also act in favour of refinements in time and pseudo-time behaviour. Therefore MINF makes allowance for the rock mass responding to time on three scales:

1. Milliseconds during seismic events,

2. Hours during viscous relaxation and

3. Days to years during changing mining geometry.

2.3 EO3: Presentation of a preliminary report and motivation towards full completion of the planned project.

The project proposal included this enabling output because it was originally submitted to SIMRAC as an ad-hoc proposal and this output was included to provide an easy way for SIMRAC to critically judge progress on this work during the first year before agreeing to support a second year of study. The motivation was presented in September 2000, after which approval was given full completion of the project.

2.4 EO4: Illustrate within selected areas and through back-analysis that changes in seismicity are generally more accurately estimated from changes predicted by modelling when parameters are calibrated from previous mining and seismicity

The development work on MINF that took place under this project for SIMRAC benefited from the application on MINF to the case studies done for the Deepmine collaborative project, Task 5.2.1, “Integration of modelling and seismicity”. In this project, modelled cumulative seismic moment and frequency-magnitude distributions were compared to the observed data. By adjusting the strength values that are described in Chapter 3, it was shown that observed data could be well approximated by modelled data. In particular, changes in the observed event rate were well accounted for, as reported in Chapter 8 for two of the four case studies reported by Nxumalo (2001). Instead of duplicating efforts by doing more case studies for the current (SIMRAC) project, we learned about the sensitivity of the modelling to different parameters from the results of the Deepmine work. The time saved was spent on making more progress within other areas of work in this project.

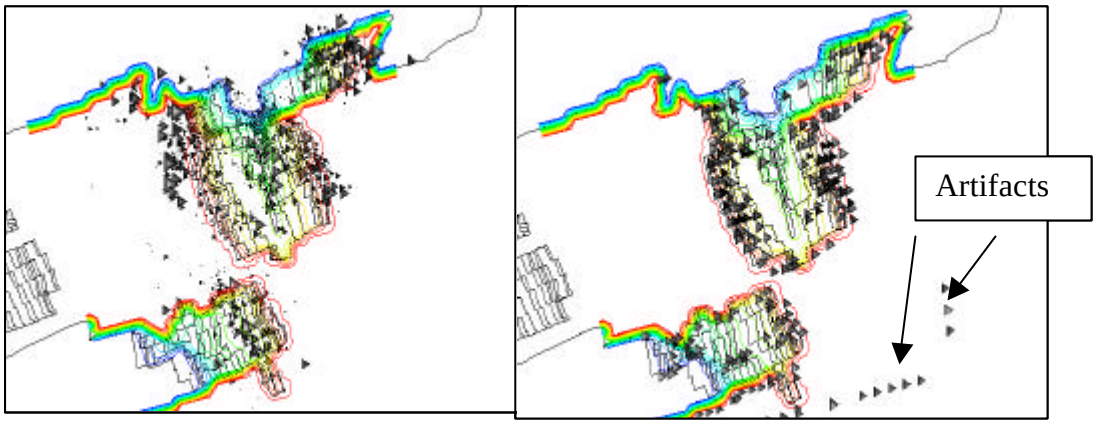

Figure 2-2. Plot of seismicity on a digitised plan at TauTona. Mining steps as contours. Observed seismicity on left and modelled seismicity on right.

A keynote address entitled: "Synthetic seismicity mimics observed seismicity in deep tabular mines" was delivered at the 5th International Symposium on Rockbursts and Seismicity in Mines, on September 20th 2001. The paper is included here as Chapter 8.

From the beginning, the MINF code has employed a direct simplification in allowing for failure of the rock mass. Most of the mine-wide modelling has taken place by considering one component of stress only, namely the stress normal to reef. Although the program has generated seismicity catalogues with properties very similar to observed seismicity catalogues, efforts to eliminate certain deficiencies have not been totally successful. These have included approximations for strain hardening on squat pillars and some approximations for confining stress.

2.4.1 Towards fully 3D spatial modelling

It has been a long-term objective of the development of the MINF code to move into true three-dimensional deformations and we took the opportunity of using a Miningtek bursar to assist in setting up the mechanisms for defining the functions that relate stress to DDs (Displacement Discontinuities) on a cubic array of elements. This is a complex multi-dimensional problem. Figure 2-3 below is a sketch that illustrates an addressing system that could be used. The basic elements are the three faces that are at positive values along X, Y and Z.

The classic on-reef problem is solved in terms of the base element "A" repeated along a large number (e.g. 64 or 128) of elements along X and Y. As reported before by Spottiswoode (1997), reef-parallel (bedding-plane) shear can be handled by elements parallel to the stope elements. The ability to allow for shear slip on planes normal to reef will be the major feature of new developments. Shear slip nearly normal to the plane of the reef is the most widely recognised mechanism for mine seismicity.

In comparison to generalised 3D codes, MINF will retain the regular structure that is used by MINSIM and MINF. By keeping to powers of two along X and Y (NX and NY elements) and small numbers of vertical cells (NZ << NX and NZ << NY), the regular structure allows for storage of influence coefficients of size $NX \times NY \times NZ^2$. Through vertical lumping, this could be further reduced. Numerical motivation for this approach can be seen in Figure 2-3 and Figure 2-4. Work along this line will continue in the new SIMRAC project (SIM 02-03-01) under the leadership of Dr J.A.L. Napier in 2002 to 2005.

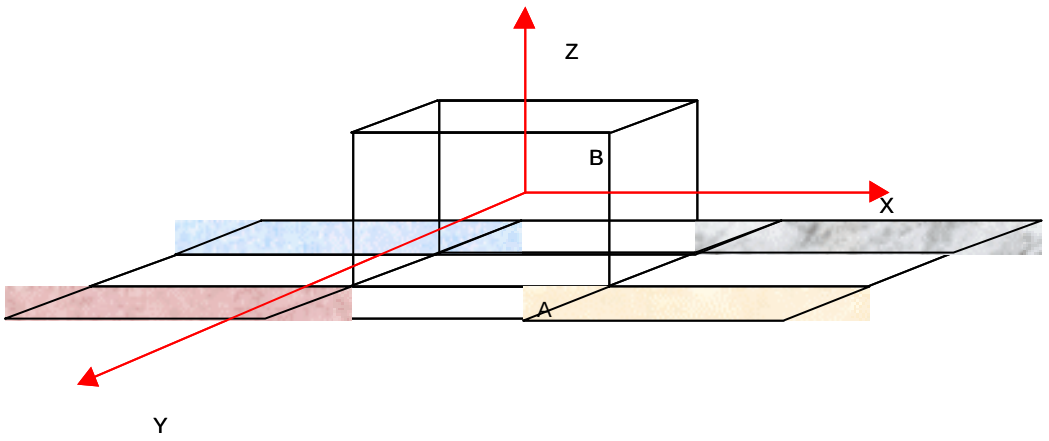

Figure 2-3 A unit cube in 3-D space for 3D MINF. The X-axis represents column numbers along strike and the Y-axis row numbers down dip, according to the numbering system used by MINSIM.

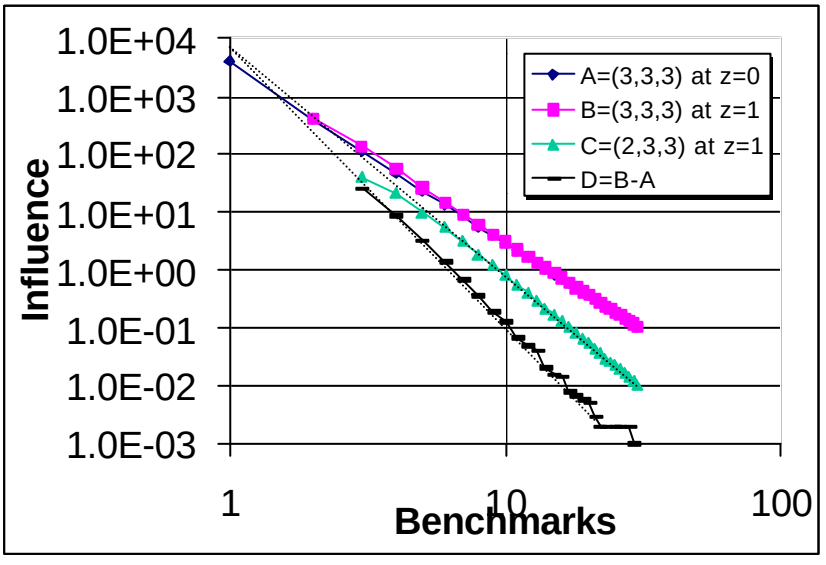

Figure 2-4 Faster fall-off of influence values and differences between layers support "lumping" of values along X and Y beyond 10 times differences in Z. A, B and D refer to normal stress from a normal DD. C is the shear stress. This can be used for massive reduction in computer run times.

2.5 EO5: Industry workshops to train rock mechanics and seismologists in the use of the software.

A CSIR internal workshop has taken place as part of a MinSim2000 workshop.

Preliminary documentation for MINF has been written and is presented in Chapter 5. The structure of the main input data file has been described and provides for many options. However, the program is complex and it is convenient to treat its functionality as if it consisted of three independent programs:

1. **MINF_MEGA**. This code is suitable for running solutions of elastic problems on a single plane, with or without cap stress, using up to 1024 by 1024 elements. The direct elastic solutions are necessary for testing and calibration against known solutions.

2. **MINF_MULTI**. Multiple parallel planes. Applications would be mining of the Merensky and UG2 platinum-bearing reefs, for example to look at interaction between pillars. Also shallow coal mining with bedding-plane slip and soft seams.

3. **MINF_SEISMIC**. This is the "engine" for synthetic seismicity simulation presented in this project.

This partitioning allows the user to progress in stages from simple single-reef problems, through multi-reef problems before handling the more complex seismicity simulation.

The code for the "**MEGA**" solver is changed in parallel with the "**MULTIi**" and the "**SEISMIC**" solvers so that the "**MEGA**" solver is always available for calibration of the vastly more complex "**MULTIi**" and the "**SEISMIC**" solvers. This is very useful for code maintenance and testing. All three solvers provide the same on- and off-reef deformations for simple single-reef solutions.

At present it is only **MINF_Seismic** that is the formal deliverable to SIMRAC, although the program does all three options. The actual delivered program provides for three parallel planes and 256 by 256 elements, sufficient to run small models of the "**MEGA**" and "**MULTI**" options. Larger models for each option requires customised source-code compilation.

Deepmine courses on seismic management were presented in October and November 2001 that included lectures on the topics of:

- "Critical assessment of parameters used as indicators of seismic hazard (APS, ERR, ESS etc)"

- “Integration of seismic monitoring and numerical modelling: the CSIR MINF approach – methodology and results”.

In these courses, DEEPMINE assisted in transferring to the industry much knowledge obtained by SIMRAC, in the current project and other projects. The response received during these presentations will help direct the format of the industry workshop to be held on 20th May 2002.

2.6 EO6: Consolidation of the above work into a final report.

This report meets this Enabling Output.

3 Rock strength, seismicity generation and time-dependent behaviour.

This Chapter is an edited and enlarged version of the section on "Mimicking seismicity" in Chapter 8, which is retained for consistency.

3.1 Space and time history of mine seismicity

Rockbursts have been associated with deep-level mining in South Africa for as long as deep mining has taken place. By using data from the first underground network of geophones, Cook (1963) documented the close association in space and time of mining-induced events with the advancing faces, with the event rate decreasing with time after the blast. Ortlepp (1978) recorded the appearance of two complex shear zones created during two (or more) seismic events, as exposed in a specially developed raise. When geological discontinuities, such as faults and dykes, abound and control the mining layouts, the largest seismic events occur through slip on these features (e.g. Gay et al 1994). The dominant mechanism of deformation is therefore shear slip on either mining-induced or geological fault planes. In all cases, a combination of rock strength, the imposed stress and time-dependent effects control the seismicity.

Once a shear plane has been formed, the shear strength of this plane is controlled by the slip history and has been shown to depend on the slip rate and thickness of gouge. Marone (1998) pointed out that the shear resistance of fault gouge reduces when the slip rate increases and that the gouge strengthens with time through compaction during normal loading.

Numerous papers on seismicity simulation have appeared since Burridge and Knopoff (1967) studied the concept of a spring-slider stick-slip model. Shaw and Rice (2000) were able to simulate earthquake sequences through repeated dynamic shear slip on a single fault plane. This might suffice for earthquakes occurring on a single identified fault, but mine seismicity takes place in three spatial dimensions. Problems that involve three spatial dimensions are generally addressed in terms of quasi-static behaviour, with limited consideration of time (Napier, 1998 and Lyakhovsky et al, 2001). These studies were therefore limited to inelastic effects in three dimensions, either two spatial and one time or three spatial dimensions.

As discussed in the previous Chapter, mines aim to control mine seismicity through layout design based on minimising ERR, APS and ESS. ERR does not consider rock strength at all, use of APS suggests that pillars have a certain strength that should not be exceeded, while

current use of ESS allows for a limited amount failure. In these cases only one value of strength is applied.

3.2 Four states of rock strength

Napier and Malan (1997) used two values of strength, unmobilised and mobilised, to approximate the behaviour of intact, or failed rock, respectively. They were able to simulate both time-dependent fracturing and seismicity in brittle rock. Malan (2002) showed that the time-dependent behaviour of rock, in the absence of seismicity, could be approximated using **two** material strengths; a strength of the **intact** rock that may never be exceeded and a **final**, or **mobilised**, strength to which the material tends in the long-term through a viscoplastic process. With the unfailed material behaving in an elastic manner, the overall behaviour of the rock mass can then be described as viscoplasto-elastic. He showed that this model could be used to explain observed time-dependent behaviour.

Malan's (2002) approximation does not allow for sudden drop in strength during a seismic event, whereas Napier and Malan (1997) assumed that there was one single final value of strength, whether achieved through seismic slip or slowly through viscous creep. As we saw from the previous section, this strength drop involves elements of time and velocity for slip on predefined planes. In the case of mine seismicity, we must deal with either predefined planes or previously intact rock. A further consideration is the reduction in strength that occurs during seismic failure. This may be described by the dynamic coefficient of friction. We must have (at least) **three** values of rock strength to generate and control modelling of seismic events; the strength of **intact** rock, the post-failure strength under **static** conditions and the strength during **dynamic** conditions when slip occurs.

Combining the **two** strength values from Malan (2002) and **three** strength values to approximate a seismic event, leads to (at least) **four** strength values to describe both seismicity and viscous-type behaviour. Note that the intact strength is common to both models of rock behaviour.

Rock strength is approximated here in terms of four states:

1.) **Peak** strength of **intact** rock, such as that measured during triaxial testing of samples of rock.

2.) **Static** strength of previously failed or fractured rock. This might consist of a combination of cohesive strength of partly failed material and also the internal static friction.

3.) **Dynamic** strength as the load-carrying capacity of the rock during a seismic event. This might relate to the dynamic coefficient of friction.

4.) **Final** long-term strength after time-dependent weakening has taken place. This is also termed "**mobilised**" strength by Malan (2002).

The stress drop that drives seismic events can be obtained by stress drops from either states 1 or 2 down to state 3. Through a simple viscous law (e.g. Malan, 2002 and Malan and Spottiswoode, 1994), the decay to state 4 can simulate the time dependent behaviour of rock.

Table 3-1. Summary explanation of meaning of the four rock strengths, and supplementary properties, as applied in MINF.

Parameter name in code	Description	Default value[2]
UCS_p	**Peak** strength (such as from triaxial test). When this is exceeded, stress drops "seismically" until the stress reaches "_d".	250 MPa
UCS_s	**Static**, post-seismic strength (strength of failed rock). Strength after failure. When the stress is brought back to exceeding this stress, the stress drops "seismically" until the stress reaches "_d".	200 MPa
UCS_d	**Dynamic** strength due to seismic overshoot (as in dynamic friction). Strength to which grid points relax during seismic events.	199 MPa
UCS_r	**Residual**, post-viscous strength (long-term strength), to which grid points relax during viscous relaxation.	150 MPa
UCS_g	Strain hardening gradient, applied to all four strength states.	800 MPa/m
fac[3]	Confinement strengthening: Strength = UCS + fac * σ_{Hmin}, Where σ_{Hmin} is the minimum stress parallel to the plane of the reef.	0.0
zp(2)	Distance from reef at which σ_{Hmin} is calculated. Only relevant for fac > 0.0	30 m
visc_s	"Surface viscosity"	50 000 MPa-hour/m

[2] Note that the default values are only suggestions, based on simulations that have given some "reasonable" results. Each individual case might work "best" with different values. Changes of these parameters will result in changes to the amount and character of seismicity and time-dependent effects in a complex way that is still not understood.

[3] This factor was introduced in an attempt to take confinement into account. Its effect has not been well studied and it is suggested that this factor is not used at this stage. In that case, it is appropriate to set zp(2) = 0.0.

Most of the work done to date using MINF has been done though implementation of these strength concepts.

Spottiswoode (1999) showed that simulated seismic catalogues could have generic characteristics similar to observed seismic catalogues. Spottiswoode et al (2001) performed case studies using data from several mines. Firstly, though, a short description of the method of event simulation is needed here. The reader is referred to Chapter 6 for more details of the Boundary Element numerical code used (MINF).

3.3 Simulation method

Once the mining geometries and sequences have been defined and the rock strength specified, the MINF code functions as follows, with reference also to Table 3-1 and Figure 3-1. In the current analysis, simple one-dimensional strength descriptors are applied in which only the normal on-reef stress is considered.

1. Remove rock through stress relaxation on elements that are currently being mined. As element sizes are typically much larger than the face advance per blast (typically 10m and 1m respectively), stresses on the elements to be mined are reduced in stages, say 10 in this case.

2. Test every unmined element for possible seismic failure. Seismic failure is initiated at the point at which the strength of either failed or unfailed rock is exceeded by the greatest amount. When this element fails and the stress redistributed, the immediate spatial neighbours with stress exceeding their strength are also allowed to fail. This process is repeated until no further slip occurs. The event growth is stopped when all neighbours are either too strong or have previously lost too much strength due to seismic overshoot or viscous post-failure relaxation. During the growth process the normal stress transfer from yielding elements onto all other elements, as provided by the Boundary Element Method, takes place. Repeat this process until no element has a stress value greater than its strength and therefore no further “seismic” failure is possible. In this case, continue to step 3.

3. Move forward in time a fraction of the time between face advance steps and allow viscous relaxation in proportion to stresses exceeding the final, long-term, strength. Go to step (1) if the next face advance is due; otherwise go to step (2) to test for possible seismic failure.

Each “event” can be described by the same source parameters as those used to describe observed data:

- The location is the point of initiation.
- The time is provided by the representation of the mining history and the time after the most recent face advance, or face “blast”.
- The seismic moment is equal to the product of the modulus of rigidity and the “volume” of seismic deformation given by the summed Displacement Discontinuity (DD), as shown in Figure 3-1, multiplied by the area of each element. In the case of the normal stress and DDs, as simulated here, a correction should be made for equivalent inclined shear slip.
- Seismic energy is estimated from the work done on each element in excess of the dynamic strength. It should be noted that negative energy release on individual elements is possible when slip occurs but the stress after the event is greater than the stress before the event. The overall energy release is, however, always positive.
- In the normal manner, other source parameters such as moment-magnitude and apparent stress are determined from the seismic moment and seismic energy.

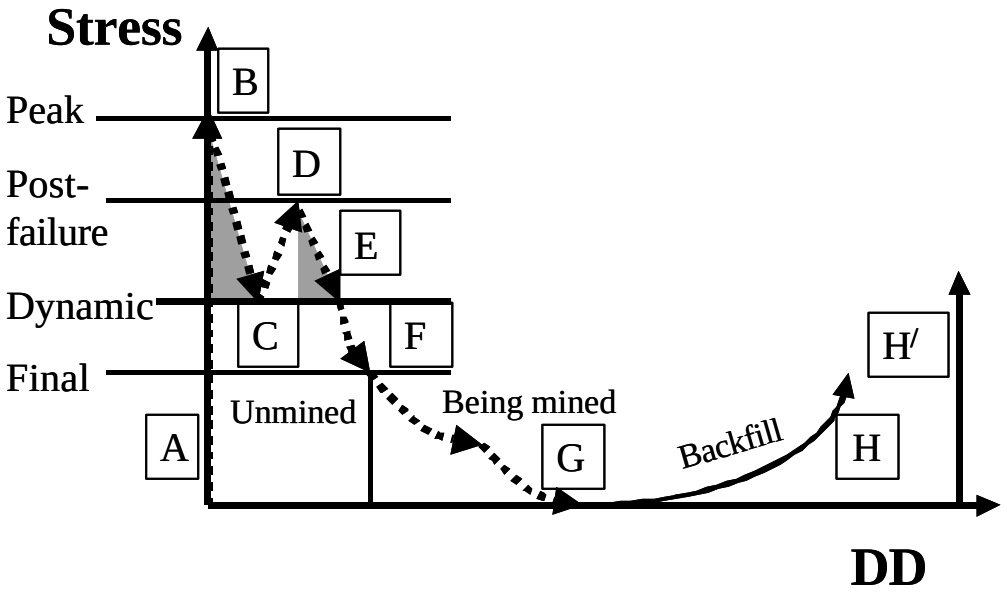

Figure 3-1 Cartoon illustrating a simplified stress-deformation history of an on-reef element in MINF

Stress increases from virgin stress (A) to the ultimate strength of solid rock (B) as mining advances. Failure occurs and the stress drops along the load line (C), generating a simulated seismic event. Nearby mining or seismicity might increase the stress sufficiently again to initiate another seismic event (D) and the stress drops again along the load line to (E). With time, the

stress may drop further to the viscous, long-term, strength (F). When this element is mined in stages at the face, the stress relaxes viscously with time and instantly with mining step to zero stress (G), with two stages of stress relaxation illustrated here. Finally, the stress may build up on backfill (H) or when convergence is complete ($H^{\prime}$).

The history of stress and deformation of a grid element can follow many different trajectories. Figure 3-1 illustrates one such directory:

A-B: Increased stress from the virgin stress, A, as mining approaches this point. This is the same behaviour as would be simulated by MINSIM.

B-C: Failure and stress drop along the load line when the peak strength at this element is exceeded. This results in a simulated seismic event involving this element and perhaps also other, contiguous elements.

C-D: Stress increases through mining of nearby elements and through nearby seismic events.

D-E: Seismic stress drops if the point D falls above the post-failure strength line.

E-F: Viscous stress relaxation of this element with time.

F-G: The element is now mined out, through zonking if applicable.

G-H: The stress may then increase along the backfill strength line, if applicable. In the case of complete convergence, the stress build-up occurs without further convergence and the stress-DD history follows **G-H**$^{\prime}$.

The crosshatched areas are used to characterise the contribution of this element to each of the two events, with the base contributing to the seismic moment and the area to the “radiated” energy. The second “seismic event” is included to account for cases of remobilisation as part of an event that initiates nearby. Each failed element may be involved in one or more seismic events.

The current analysis methodology is strongly affected by assumptions regarding the “strength” of pillars and unmined ground. It is biased in favour of mine layouts with low extraction ratios. Nonetheless, the MINF program provides some insights into magnitude distributions and possible incidences of strong ground motion for the conceptual layouts evaluated here.

The above-mentioned *strengths* are implemented as follows:

1. ***Remove rock at the fixed times*** - each element being mined is relaxed in KZONK steps. This is similar to the so-called *zonking* in FLAC™ and incrementally reduces the amount of load transferred from the face elements.

2. ***Test every element for possible seismic failure if its strength is exceeded*** - seismic failure takes place when stresses exceed the strength of intact rock or, for failed elements, the quasi-static strength of failed rock. Seismic failure is initiated at the element with highest excess stress above these strengths and is allowed to grow to any of its spatial neighbours for which the stress exceeds the strength. In two dimensions, the user may ask MINF to search the four neighbouring elements with a common edge or the eight neighbouring elements with a common edge or point. In the three-dimensional case, this expands to six or twenty-six.[4] The failure region is allowed to continue expanding until it is surrounded by either mined-out ground or unmined ground with stress less than its strength. Repeat this process until no *seismic failure* is possible anywhere.

3. ***Allow viscous relaxation according to Equation*** (3-1) for all failed elements with stress in excess of the ultimate strength. If the next face advance is due (i.e. when 24 hours is up, go to step 1). Else, return to step 2) to test for possible seismic failure.

In the MINF models run, viscous creep takes place on failed elements in response to σ_e, the stress in excess of the final strength as follows:

$$dDD = dt * s_e / V \qquad (3\text{-}1)$$

where *dt* is the time step and *dDD* the corresponding amount of deformation, either normal to reef in the case of the rock mass or in plane, and *V* is the surface viscosity. A single element that moves according to Equation (3-1) behaves as

$$d \sim e^{\frac{-t * S}{V}} \qquad (3\text{-}2)$$

where d is the deformation (crush or ride) and S is the self-effect. The time step was chosen as dt = 0.20 * V / S so that the exponential decay could be adequately followed.

It assumed that the parameters introduced in MINF were physically reasonable; supporting simulations that result in numerically- generated outcomes similar to *in situ* observed responses.

The "z*onking"* functionality designed in MINF is aimed at reducing the increment of stress imposed on the unmined elements during any single mining step.

[4] The number of immediately adjacent neighbours is 2×D, where D = Number of dimensions (2 or 3). The number negbours, including those with a common point, is 3^D-1.

Lastly, some tests have been made on adjustments to the strength laws through strain hardening and foundation clamping. In addition, a stress overshoot by a factor of UCS_F from pre-seismic stress beyond the “dynamic” strength UCS_d has also been considered. These adjustments are briefly described in the documentation on the code in Chapter 5. More follow-up work on these concepts might follow in 2002 or 2003.

4 MINF program and sample data.

The MINF program as at 15th April 2002 is available for immediate use in the electronic version of this report through a hyperlink to the executable file MINF.EXE if the following files are placed in the same directory as this document. Please check that the "read-only" attribute in "file properties" is switched off if the files have been read from CD or the Internet. The description of each file is hyperlinked to the appropriate section of this report. For full use of MINF, "*demo*" can be replaced by *prob* = your problem name, as described in Chapter 5. Figure 4-1 Flow-chart illustrating how to run MINF.is a flow diagram for running MINF.

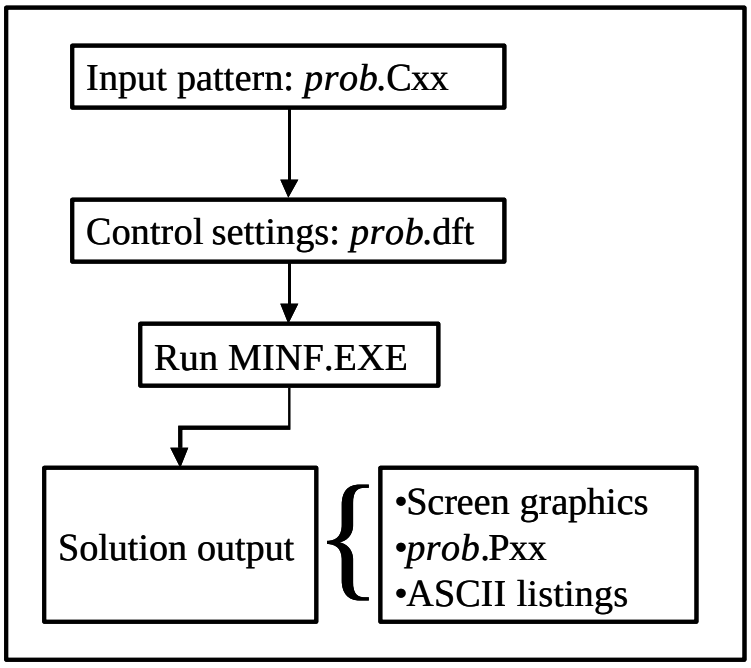

Figure 4-1 Flow-chart illustrating how to run MINF.

MINF.exe

This is the DOS™ executable. MINF has not yet been able to access the name of the "current directory" which sometimes deviates from the directory in which the project files are installed. In this case the program will require an input for the prompt "Enter problem description:". In this case, the program should be run as MINF in a DOS window in the correct directory. When the program has completed the solution, the user must return control to Windows™ to return to this document. If you see the following screen (Figure

4-2) on completion of the program, please select Y for “Yes” to release the DOS™ window

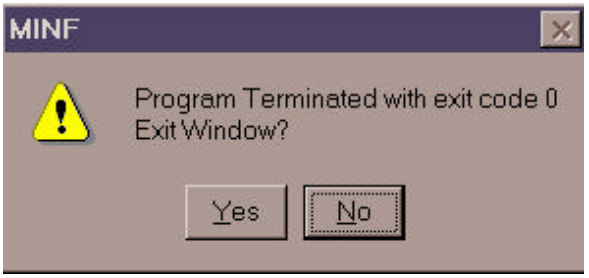

Figure 4-2. Windows message on termination of MINF DOS program.

Demo.ci0

This file represents a small sample mining pattern with 32X32 = 1024 elements, simulating the mining of two raises. It is supplied to provide immediate access to MINF. Refer to the user manual in Chapter 5 for use of MINF with different MINSIM “Cxx” file(s).

In addition, the following ASCII files are advised, but are not compulsory:

Demo.dft

Control file for the *demo.*ci0 file. The attached *demo.dft* file results in a seismicity simulation.

This sample MINF run should take 15s on a 1GHz PC. Some simple DOS graphics shows the time stepping of mining and seismicity and ends with the screen shown in Figure 4-3. . If this file (demo.dft) is excluded, the program is run as a 5-step elastic simulation and takes two seconds to run to completion. Conversely *zooming* and *zonking* can be used to provide a more detailed rock mass response and the program will take longer to complete (151s). The final screen picture for all three options mentioned here are presented in the attached file MINF_DEMO.ppt.

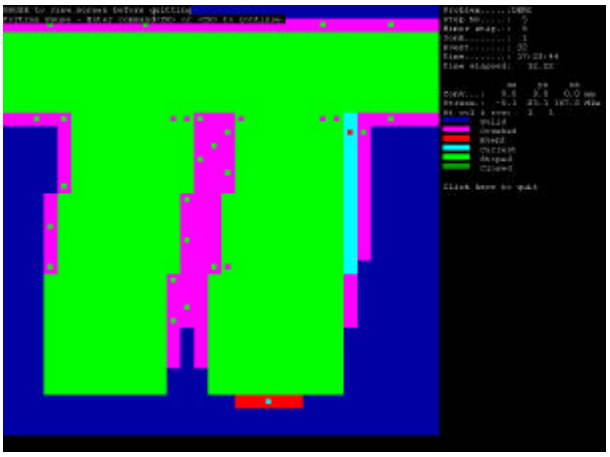

Figure 4-3 Screen on termination of MINF with sample “demo” data.

MINF_dft_help.txt

Documentation that is wrapped around the raw form of the *demo*.dft file, as described in the next Chapter.

5 User manual for MINF & associated programs.

5.1 Description of MINF

These programs have been integrated as a suite to test the concepts and criteria mentioned above by doing large-scale back-analyses of mining and seismicity. Large-scale means shaft-sized. The major thrust in the development of MINF has been the capability of simulating seismicity in time and space.

MINF is a MINSIM-type boundary element solver for large numbers of grid elements on a single reef. It reads MinSim2000 pattern files for one or more co-planar coarse files. MINF operates in several different modes. The following list contains the currently valid modes of operation.

5.1.1 MINF_MEGA

Single reef with cap stress and no seismicity generation. This option can use up to 1024 by 1024 elements.

5.1.2 MINF_MULTI

Multi-layer model, consisting of a single reef with reef-parallel layers that simulate the free surface or allow shear slip.

5.1.3 MINF_SEISMIC

Reef and parallel layers with seismic and viscosity generators.

Unless otherwise stated, the programs use units of megapascal (MPa) for stress and metres (m) for convergence, ride and displacement. Compressive stresses and stope closure DD's are positive.

5.2 Description of associated programs

The MINCON, MINFLIST and MINFSUM programs were written as service programs for MINF. MinView3D is a commercial program that is part of the MinSIm2000 suite. Substantial structural changes are planned for these programs. Nonetheless, they are briefly described here.

5.2.1 MINCON

MINCON smoothes the grid pattern of deformation parameters. It also grids and smoothes seismicity. MINCON appends "~" onto the binary files Pxx files and writes *prob*~.Pxx files.

The main motivation for MINCON is the need to relate each seismic event directly to the mining that caused it. This should sharpen, or localise, the spatial relationship between cause and effect.

5.2.2 MINFLIST

Lists output data in ASCII form that complements MINXL.

5.2.3 MINFSUM

Writes summary values of mining parameters such as energy and observed (or modelled) seismicity by area to ASCII output files.

5.2.4 MinView3D

MinView3D is a Windows-compatible commercial product that was written specifically for displaying the "Pxx" output files of MinSim2000, together with mine outlines (MLS) and seismicity.

MINF, MINCON, MINFLIST and MINFSUM are DOS programs and run as:

PRNAME

or

PRNAME [*prob*],

Where PRNAME = MINF, MINCON, MINFLIST or MINFSUM

and *prob* is the problem name as used in the MinSim2000 pattern files, *prob*.ciN or *prob*.cNN. *prob* contains up to 6 ASCII characters.

When *prob* is not entered in the command line, the user must provide it through a prompt. When the file *demo*.ci0 is found on the current working directory, MINF will not prompt for a problem name (*prob*), but simply set *prob* = “demo” and work with the *demo*.ci0 file. All user-defined parameters are contained in the file *prob*.DFT, described below.

5.3 List of files

5.3.1 MINF.EXE

This is the MINF DOS™ executable. It may reside in the same directory as the input files listed below. However, for better use of directories it is recommended that MINF.EXE be kept in a separate directory (e.g. “C:\PROGS” or “C:\MINF”), in which case this directory name must appear in the “PATH =” statement in the AUTOEXEC.BAT file.

5.3.2 *prob*.CIx or *prob*.Cxx

These are compulsory MinSim2000 files containing the coarse mining pattern for mining (time) step = “x” or “xx”. If MINF is run through Windows™, this data file must be in the same directory as the MINF.EXE program. It is better, however, to use a DOS window in the directory in which this file is placed, for example: C:\MINF\SHAFT#1. All files listed from here will reside in this directory. It is called the “working directory”.

MINF also reads certain extensions to this file structure. Five additional “verbs” are available for use by MINF: “**CRCH”, “BKFL”, “SEAM”, “MULT”, “VZZ=**” and “**SMX=**”. They work as follows.

5.3.2.1 CRCH ncrch, ncrch_x, ncrch_y

ncrch = number of columns & rows (16, 32, 64, 128 etc)

ncrch_x, ncrch_y = start at this top left corner address (optional, with default = 1,1).

This verb provides a much easier way of doing multi-step mining for hypothetical mining patterns than the standard MinSim2000 multi-file method. It is based on the input file structure used by the program FREEF that was developed by Prof. S Crouch in the 1970's.

5.3.2.2 BKFL c_bkfl, sw_bkfl, a_bkfl, b_bkfl

Hyperbolic backfill, where $\sigma_z = a\varepsilon / (b-\varepsilon)$ and $\varepsilon = D_z$ / Stope width.

Table 5-1 Description of backfill variables

Variable name	Description
c_bkfl	A blank (" ") indicates that the backfill is placed everywhere A non-blank character refers to the CM pattern in the MinSim2000 "cxx" input file.
sw_bkfl	Installed fill height (m). At this stage, the stope width must be used. If it is not, an error message will be generated and the program will terminate.
a_bkfl	"a" value
b_bkfl	"b" value: must be between 0.1 and 0.9.

5.3.2.3 SEAM seam

Seam modulus as applied to problems typical of coal mining using:

$\sigma_z = SEAM * D_z / S_W$

where σ_z = Stress normal to reef

D_z = convergence normal to reef

S_W = Stope width, normal to reef.

To be used, the value of **SEAM** must be > 0.0 MPa.

5.3.2.4 MULT ix_off, iy_off

Used for positioning multiple adjacent coarse windows. Before any zooming (nzoom in .DFT), this is the position of the TLHC (Top Left Hand Corner) is at (column, row=) ix_off, iy_off. It is assumed that ix_off, iy_off = 0,0 for first window. Ix_off and iy_off must therefore = N*64, where N is a small integer. This is an obsolescent feature as MinSim2000 allows for digitising of windows with >64 grid elements in each direction.

5.3.2.5 VZZ= nvzz1, nvzz2, nvzz3 (integers)

Loops over VZZ (in MPa) from NVZZ1 to NVZZ2 in intervals of' NVZZ3. Gradients are ignored and all components are scaled to the same k-ratio. This option was developed to look at the effect of cap stress on increasing depth or APS. Only one mining step (number 0) is considered and the code uses further steps to simulate changes in VZZ.

5.3.2.6 SMX= NSMAX1, NSMAX3, NSMAX3 (integers)

Loops over SMAX (in MPa) from NSMAX1 to NSMAX2 in intervals of NSMAX3. This option was developed to look at the effect on convergence of decreasing the cap stress. Only one mining step (number 0) is considered and the code uses further steps to simulate changes in SMAX. The program cannot have both the VZZ= and the SMX= commands.

5.3.3 *prob*.DFT

Data file containing values of parameters that MINF needs and that are not provided in the MinSim2000 “cxx” data files. It is needed for MINF, MINCON, MINFLIST and MINFSUM. Changes to all fields must be effected with an ASCII editor, such as Microsoft® Notepad™.

This file uses the fortran NAMELIST construct, in which variables are given values. On its own, this form is bare and provides no direct help in its use. However, MINF contains a custom-written utility that wraps descriptions of the variables and groups of variables around the bare form of the *prob*.DFT file so that it becomes self-documented. This file will be created with default values if it does not exist.

5.3.4 MINF_DFT_HELP.TXT

Documentation file that is wrapped around the bare *prob*.DFT file. This file should reside in the root directory (c:\), but may reside in the current working directory.

5.3.5 *prob*.Pxx

Binary files containing the solutions for mining step number “xx”. Generated by MINF and used by MINCON, MINFLIST, MINFSUM and MinView3D.

If >=100 mining steps are considered, steps 100 to 998 are given the name: ***probn.*pyy**, where n = (step number / 100) and yy = (MOD(step number, 100)).

5.3.6 *prob*9.P99

Binary files containing the virgin stress field, mining pattern and energy release summed over all mining steps. Generated by MINF.

5.3.7 *prob*#.Pxx

Binary files containing the off-reef stresses and displacements. Generated by MINF when sheets are requested (NP > 0 in *prob*.dft)

5.3.8 prob~.Pxx

Scalar values written by MINCON and used by MINFLIST, MINFSUM and MinView3D.

5.3.9 ?.txt or ?.?

List of observed seismic events. Synthetic or observed seismicity to be read by MINCON and MINFSUM. The TXT extension indicates that the seismic data are in a tab-separated text file, with headings described below. The file name must be provided in the *prob*.DFT file under “FNSEIS =”. The same format is read by MinView3D. If the file does not have a TXT extension,

then it is assumed to be in the same format as the binary EVENTSUM file in the obsolescent PSS DOS database structure.

5.3.10 *prob*.XY4

A list of rectangles (first-to-last column and first-to-last row) for identifying areas for which seismic and mining data will be summarised by MINFSUM. Each rectangle to be preceded by the zoom level at which it was defined. Following these data, each area may be given a description, starting with "!" after the value of the last row. For compatibility with MinView3D, the columns and rows are read in the range 0 to 63 for zoom=1, 0 to 127 for zoom=2, etcetera.

This file restricts the chosen areas to be rectangles. At some stage, this file will be made redundant and replaced by a file containing coordinates of polygons.

Example:

```
2 7  74   9 126   ! E2

2 1 120   1 120   ! Almost all
```

5.3.11 General-purpose ASCII output files.

These files trace the progress of the programs, from reading the input data, through the solution stage to writing output files.

***prob*.out:** For MINF

***prob*.smt:** For MINCON

***prob*.gut:** For MINFLIST

***prob*.sul:** For MINFSUM

***prob*.sum:** Tables of convergences and stresses, from MINFSUM

Also various .TXT files as listed in table 2 below.

5.3.12 *prob*s.txt

List of all seismic events with headings, in the same format as read by MinView3D. Synthetic seismicity is written by MINF. Synthetic or observed seismicity is read by MINCON and MINFSUM. The file name is listed in the *prob*.DFT file and used by MINCON and MINFSUM.

5.3.13 *prob*nnn.txt

List of seismic events in time step “nnn” in the same format as the *prob*s.txt file. Synthetic seismicity is written by MINF. Synthetic or observed seismicity is read by MINCON and MINFSUM.

5.3.14 *prob*_1.txt

Summary of volume change and energy release at each step.

5.3.15 *prob*_1.txt

Detailed listing for seismic events.

5.3.16 zzaNNNN

Temporary binary file used by MINF. They are deleted when the program terminates normally. If the program has been abnormally terminated by power failure or by ^{Ctrl}C, then these files are retained on disk and must then be removed manually.

Table 5-2 Usage of files.

	Used by, with “R” = read and “W” = write			
File name	MINF	MINCON	MINFLIST & MINFSUM	MinView3D
Prob.DFT	R/W	R/W	R	-
*prob.*Clx *or prob.*Cxx	R	R	R	-
Prob.Pxx	W	R	R	R
Prob~.Pxx	-	W	R	R
Prob#.Pxx	W	R/W	R	R
?.?	-	R	R	-
?.TXT	W	R	R	R
Prob.XY4	-	-	R	-

Table 5-3. A list of component names and meaning. The number of parameters written might vary from 0 to 6, in order listed.

Component name	Description	Name in DFT file
DZZ, DYZ, DXZ	Ride & Convergence	NCON
SZZ, SYZ, SXZ, SXX, SXY, SYY	Stress	NSIG
SIG1, SIG3, SIG2	Principal stresses	NPSTR
UZZ, UYY, UXX	Displacements	NDISP
CENT	Energy release at this element	- (always written)

5.4 File formats.

Information will be made available using the following files, in which *problem* is the problem name (up to 6 characters long).

5.4.1 File *prob*.cxx

Here is the *demo*.ci0 file that provides the mining information for the sample MINF run.

5.4.1.1 Sample listing

```
CRCH 32
HEAD C <none> Date=01/01/00 Mineplan=<none>
PARM 1 0 15 1.500 0.200 15
CNST 20.0 0 0.200 70000.000 I
VIRG RH 0.0 0.0 0.0 0.000 0.000 0.000 40.000 40.000 80.000 0.000 0.000 0.000
CWIN C1 10.000 19.000 0.000 0.0 0.0 3000.0 0 0.500 0.000 0.200 0 0
CP 1.............................
CP 2.............................
CP 3000000000000000000000000000000000
CP 4000000000000000000000000000000000
CP 5000000000000000000000000000000000
CP 6000000000000000000000000000000000
CP 7000000000000000000000000000000000
CP 8000000000000000000000000000000000
CP 9.....222133333...554155555......
CP10.....222133333...554155555......
CP11.....222133333...554155555......
CP12.....222133333...554155555......
CP13.....222133333...554155555......
CP14.....222133333...554155555......
CP15....222213333...5555155555......
CP16....222213333...5555155555......
CP17....222213333...5555155555......
CP18....222213333...5555155555......
CP19....222213333...5555155555......
CP20....222213333...5555155555......
CP21...222221333...5555415555.......
CP22...222221333...5555415555.......
CP23...222221333...5555415555.......
CP24...222221333...5555415555.......
CP25...222221333...5555415555.......
CP26...222221333...5555415555.......
CP27...222221333...5555415555.......
CP28...222221333...5555415555.......
CP29...222221333...5555415555.......
CP30.............................
CP31.............................
CP32.............................
```

5.4.2 1. File *prob*.DFT

The MINSIM pattern provides very little opportunity to control the complex operation of MINF. This ASCII file (***prob*.DFT**) provides all control of MINF and input values must be edited using a text editor such as Microsoft® Notepad. There are 27 categories of input, listed with "! [N] Heading ==========". This file consist or two parts:

1. Parameters and the values chosen for them, example: "MAXNIT = 1000". These parameters and values use the "NAMELIST" construct provided by fortran.

2. Descriptions of all the input parameters required. These descriptions are derived from a file "MINF_DFT_HELP.TXT" that must be in the C:\ (root) drive. Note that all these descriptions are preceded by "!".

The default listing below has been edited slightly from the ASCII version for more clarity in the current format. This is be followed by some interpretation of this file with respect to progressing from pure linear elastic rock-mass behaviour through to generation of 4-dimensional seismicity patterns. See also section 3 above.

5.4.2.1 Sampling listing

```
&IN_1 !
! [1] Iteration control ========================================
MAXNIT = 1000, ! (1000) Maximum number iterations.
! The solution is usually achieved in between 6 and 30 iterations for elastic rock mass with no crushing.
! Many more may be required when spans are large and deformations are allowed.
! Over-relaxation results in faster solution times.
!
OMSP = 1.20 , ! (1.2) Over-relaxation factor for each element
OMF = 0.20 , ! (0.2) Influence of DD adjustments on neighbours.
          ! This anticipates the effect of DD corrections on the next iteration.

! [2] Solution accuracy ================================================
! A low maximum error of 0.1% of the virgin stress reults in a very accurate solution.
! The solution is terminated after the maximum absolute error (in MPa) < ACC.
ACC = 0.10 , ! (0.1) Solution accuracy required (MPa)

! [3] Cap stress model =================================================
! The stress on all unmined elements can be capped, or limited to a maximum value.
! SMAX is the maximum allowable limit for the on-reef normal stress.
!  It can be used to simulate on-reef crushing and to impose an APS limit to pillars.

SMAX = 200.0 , ! (1000)  Cap stress limit (Used only for NSOL = 1 and NERR = 1)
NERR = 1, ! (0)

! [4] Filter for spectral transfer coefficients ================================
! MINF uses influence coefficients calculated in the wavenumber domain (Peirce et al 1992, Peirce 1996)
 ! To approximate piece-wise constant elements, apply sinc and additional filtering.
 NFILT = 2, ! (2) =0 for no filtering, =1 for sinc filtering, =2 for sinc and additional filtering

! [5] Solution type ============================================
```

```
! The full version of MINF with multi-plane simulation and seismicity generation requires
!  large memory requirements (RAM) in the form of numerous full (NX by NY and NX by NY by NP)
arrays.
NSOL = 3, ! (1) =1 for classic solution
        !    =2 for multi-plane solution
        !    =3 for seismicity generator

! [6] Verbosity flag ====================================================
!      for writing output to file prob.OUT
NPR = 1, ! (0) = 0 for shortest listing to .OUT file & >=1 for successively longer listings.
! A special case of NPR = 99 is used to list the influence coefficients.

! [7] Small steps =======================================================
! Explicit seismicity generation requires mining in steps similar in size to the actual face advance.
!  For deep South African gold mines, the actual face advance is about 1.0 m.
! In contrast, face positions are available monthly, quarterly or even only annually.
! The typical face advance rate is between about 8 and 15 m/month.
! This results in face advance of between 8m and 180m from one digitised step to another.
! Gridding of the mine outines to define the areas that have been mined out at each time step
!  is typically done using a grid size of about 10m,
!  which is usually smaller than the digitized face advance, but much larger than the actual face advance.

! The following three parameters: KINT, KZONK & KZOOM are aimed at simulating a finer resolution
!  than has been provided by the digitized data.

KINT = 3, ! (0) = 0 to solve for major steps only,
        !  = 1 to advance across 8 neighbouring grid blocks from major step to major step.
        !  = 2 to advance across 4 neighbouring grid blocks.
        !  = 3 to advance on breast only
        !  = 4 for updip mining only

KZONK = 1, ! (1) Number of stages of face relaxation.  Only used for KINT>0
! This is similar to "zonking" in FLAC, whereby the stress on face elements is relaxed in KZONK stages.

NZOOM = 1, ! (1) Zoom factor to be applied to each element.
! For example, for NX=NY=64 and grid size EW=10m, NZOOM=2 expands the pattern to NX=NY=128
and EW=5m.
! Each doubling (NZOOM = 2, then 4 and then 8) uses four times RAM and between 10 and 20 times run
time.
! The NZOOM^2 elements are aligned to the local face direction
!  when the MinSim2000 file uses partially mined elements.

! [8] Isolated mining ===================================================
! MINF assumed that the mining pattern repeats itself infinitely in all directions,
!  whereas most codes, such as MINSIM, assume that the surrounding areas are solid.
! In support of the approach used by MINF, it can be argued that window of interest
!  is not fully mined.
! To reduce the effect of external mining,
!  regions of unmined ground can be added adjacent to the mining pattern.
NPAD = 0, ! (0) = 0 for no padding,
        !  = +-1 for 100% padding,  e.g. 64 by 64 is expanded to 128 by 128
        !  = +-3 for 300% padding,  e.g. 64 by 64 is expanded to 256 by 256
        ! When NPAD > 0 only the original area is written to Pxx file(s).
        ! When NPAD < 0 only the original area is written to Pxx file(s).

! [9] Number of parameters written in detail ============================
! The following numbers are used to control the number of parameters to be written to PXX files.
NCON = 1, ! (1) Number of conv. & rides stored, in order: DZZ, DYZ & DXZ, DXX, DXY & DYY.
NSIG = 1, ! (1) Number of stresses stored, in order: SZZ, SYZ & SXZ, SXX, SXY & SYY.
NAPS = 0, ! (0) =1 to calculate APS of solid surrounded by mined out areas. Stored as APS.
NPSTR = 0, ! (0) Principal stresses stored, in order: SIG1, SIG3, SIG2.
NDISP = 0, ! (0) Number of displacement stored, in order: UZZ, UYY & UXX.
```

```
! [10] PPV estimates ========================================
NV_FACE = 2, ! (2) Where do you want to write estimates of PPV?
          ! =0 for no storage of estimated PPV values.
          ! =1 to write PPV estimates only on active face
          ! =2 to write PPV estimates for all faces, active and old
          ! =3 to write PPV estimates on mined-out areas
          ! =4 to write PPV estimates in entire area.

! [11] Limit output steps ================================================
! The following two variables are only relevant for simulations of a very large number of steps
!  when the solution is only needed for a range of steps.
I_MAJ_1 = -999, ! (-999) First  step stored in Pxx files (-999 for all)
I_MAJ_2 = 0, ! (0) Last step stored in Pxx file.

! [12] Growth rules for seismic events ===================================
NKGROW = 2, ! (0) =1 to grow seismic event via any one of the four edge neighbours,
          !  =2 to grow via any one of the eight edge and corner neighbours,
          !  =3 for "simultaneous" event on all elements that might fail.
          ! -ve to require at least TWO elements to start.
          !  Starting with >= 2 elements reduces the incidence of numerous, small 1-element events.

! [13] Time step =========================================================
ZSURF = 0.0000000, ! (0.0) Z elevation of surface, to be used when .XYZ file exists.
                ! (Used by Lindsay Anderson on a special data set from Harties with non-planar reef: XYZ
file).

! [15] Weekly blast cycle ================================================
TVISC = 0.0000000, ! (0.0) Time step, in hours, for viscosity (0.0=automatic)

! [14] Special adjustment for surface not at z=0. ========================
NBL = 7, ! (7) Number of days blasted out of seven.
       ! Used in conjuction with T_TIME. Use 5, 6 or 7 for 5-day, 6-day or 7-day working weeks.
T_TIME = 7*24.0 , ! (7*24.) Time steps between face advances.

! [16] Volume of history points ==========================================
! The following 6 variables are used to describe a 3-D volume of elements
!  for which a full history of values of DZZ and SZZ are written.
! The volume is limited to a maximum of 40 points, moving through X fastest, then Y, then Z.
! The values are ignored and nothing written if any value is zero.

NHXA = 0, ! (0) Smallest x value (column)
NHXB = 0, ! (0) Largest x value (column)
NHYA = 0, ! (0) Smallest y value (row)
NHYB = 0, ! (0) Largest y value (row)
NHZA = 0, ! (0) Smallest z value (plane)
NHZB = 0, ! (0) Largest z value (plane)

! [17] File type for Pxx files ===========================================
NFILE_TYPE = 0,
YEARF = 1990, ! (90) Year of first step
MONTHF = 1, ! (1) Month of first step
DAYF = 1, ! (1) Day of first step.
DEL_MONTH = 1, ! (1) Number of months between steps.

! [19] Coordinate system transform =======================================
! This option provides for translations, scaling and rotations
!  between seismic coordinate system and MinSim2000 coordinate system.
ORS = 3*0.0 , ! (3*0) Offset to agree with seismicity (MINSIM to seismic coordinate systems)
RS_M = 1.0 , 3*0.0 ,   1.0 , 3*0.0 ,   1.0 ,
NROX = 10*1, ! (10*1) Rock normal stress
NBED = 10*1, ! (10*1) Bedding shear strength
```

```
NTEN = 10*1, ! (10*1) Bedding tensile strength

! [21] Strength data-base ================================================
!  This is the "strength data-base" to be applied to each layer
!   and to dykes or faults cross-cutting the reef if defined as such in Cxx file.

!  Normal to elements:
!     UCS = 1-D strength normal to DD, MPa
!     FAC = Confinement factor from off-reef value of Sigma_h_min, add to UCS.
!           Applied when NP=1 and ZP(2) > 0.0

!  Shear or tensile strength on each plane:
!     C0  = Cohesive strength of bed, MPa
!     PHI = Friction angle, degrees
!     T0  = Tension cut-off (<0 for tensile strength)

! _P Peak (pre-seismic) stress
! _S Post-seismic Strength
! _D Dynamic strength during seismic failure
! _R Long-term Residual stength, following seismic failure and viscous creep.
! _F Overshoot by a factor of UCS_F from pre-seismic stress beyond the dynamic strength UCS_d

!  NOTE: The arrays are used in conjunction with rock types NROX, NBED, NTEN & pattern of geology.

DIL = 5*10.0 , ! (5*10) Dilation angle ??.

UCS_P = 5*250.0 , ! (5*200) Peak 1-D strength, MPa
UCS_S = 5*200.0 , ! (5*170) 1-D strength of failed rock, MPa
UCS_D = 5*199.0 , ! (5*169) 1-D dynamic strength (MPa)
UCS_R = 5*150.0 , ! (5*150) 1-D residual long-term strength

UCS_F = 5*0.0 , ! (5*0.2) Seismic overshoot

CS_G = 5*800.0 , ! (5*800) Work hardening strength (see York), MPa/m

FAC_P = 5*1.0 , ! (5*1)
FAC_S = 5*1.0 , ! (5*1)
FAC_D = 5*1.0 , ! (5*1)
FAC_R = 5*1.0 , ! (5*1)

C0_P = 5*20.0 , ! (5*20)
C0_S = 5*15.0 , ! (5*15)
C0_D = 5*14.0 , ! (5*14)
C0_R = 5*10.0 , ! (5*10)

PHI_P = 5*20.0 , ! (5*20)
PHI_S = 5*20.0 , ! (5*20)
PHI_D = 5*20.0 , ! (5*20)
PHI_R = 5*20.0 , ! (5*20)

T0 = 5*-10.0 , ! (5*-10)

! [22] Post-seismic viscosity ============================================
! Post-seismic viscous-plastic deformation may be allowed.
!  This will simulate time dependency similar to that observed after the blast.

VISC_S = 5*50000.0 , ! (5*30000) Surface viscosity, MPa-hour/m
VISC_V = 5*1.0000000E+10 , ! (5*1.0E+10) Volume viscosity proportional to DD value, MPa-hour

! [23] Layers for simulation ============================================
!  Reef-parallel plane layers to be simulated.
```

```
NP = 1, ! (1) Number of layers (watch for compiled problem size)
ZP = 20*0.0 , ! (20*0) Elevation above reef, ZP(1) = 0.0 is used for reef.

!         When NP=1 and ZP(2) > 0.0,
!          the FAC (Confinement) factor is used estimate confinement from consider off-reef skin stress.

! [24] Benchmark sheets ========================================
NBENCH = 0, ! (0) Number of benchmark sheets
ZB = 20*0.0 , ! (20*0) Elevation above reef of benchmark sheets.

! [25] Reading seismicity data ================================================
! File containing seismicity data.

! PSS EVENTSUM structure
!  OR a "TXT" extension that is assumed to be an ASCII file in the format required for MINSIM_3D viewer
!  with free format headings containing combinations of the following fields

! "EventID" as an integer number.
! "i_maj" as the MINSIM (major) step number.
! date in YYMMDD or YYYYMMDD format
! time in HHMM format
! "x", "y" and "z" OR "LocationX" etc for seismic event location
! "Mo" for seismic moment (MN-m)
! "Mo_SI" for seismic moment (N-m)
! "E" for seismic energy (MJ)
! "E_SI" for seismic energy (J)
! "Radius" for event radius
! "Taus" for static stress drop (MPa)
! "Magn" or “Magnitude” for event magnitude
! "date", "x", "y", "z" and either "Mo", "Mo_SI" or "Magn*" are compulsory

FNSEIS = "eventsum.evs    ", ! ("eventsum.evs")

DISTZ = 9999.0 , ! (9999.) Only events within this distance from reef ONE are to be considered.
FGAUSS = 50.0 , ! (50.) Gaussian smoothing distance for observed or modeled data.
EMAG_MIN = 0.0, ! (0.0) Smallest magnitude event to be considered

! It has been suggested that the source radius derived from:
! 1.) the Brune model using corner frequency and
! 2.) the MINF use of the Aki model (taus = 7Mo / 16r^3) under-estimates the source dimension
! This could also be an artifact of the MINF modeling

BRUNE_SC = 1.0 , ! (1.0) Scaling factor to increase radius of Brune-type source.

! [26] Area for extracting summary data for MINFSUM ============================
! The following data allows for extraction of summary data from one rectangular area.
! It should be replaced by the polygon outlines to be provided by Malcolm Drummond (April 2002)

NX_A1 = 1, ! (1) Left of area used for calculations of gamma.
NX_A2 = 256, ! (256) Right, largest column -- ditto --
NY_A1 = 1, ! (1) Top, smallest row -- ditto --
NY_A2 = 256 ! (256) Bottom, largest row -- ditto --
/
```

Seismic data are sometimes available in a different coordinate system from that used during the MinPlan (MinSim2000) digitising. The following transformation is used to obtain seismic X & Y coordinates from the original mining coordinates used when digitising using MinPlan:

*xorms = xform(1,1) * xorm + xform(2,1) * yorm + xform(3,1)*

*yorms = xform(1,2) * xorm + xform(2,2) * yorm + xform(3,2)*

For the trivial case of the same coordinates : xform(1,1)=xform(2,2)=1 & the other terms are zero. Note the coordinate translations in the example above.

Note : xorm,yorm,zorm = the mine coordinate values of the centre of the first element in the first row

5.4.3 Seismic catalogue files.

Seismic catalogue files, whether containing observed or modelled seismicity, describe each event in terms of its "size" using various parameters. As described in the previous section, the following parameters are recognized:

Seismic moment, M_0 (Header label = "Mo" or "Mo_SI")

Seismic radiated Energy, E (Header label = "E" or "E_SI")

Source Radius, r_0 (Header label = "Radius")

Static Stress Drop ($\Delta\sigma$) (Header label = "Taus")

Magnitude, M (Header label = "Magn" or "Magnitude")

When a seismic catalogue file is read and not all parameters are provided, missing parameters are estimated from the parameters that have been provided, according to the following rules:

1. If no seismic moment is given, assume that the Magnitude is Moment-magnitude. $M0 = 10^{9.1 + 1.5 * M}$.
2. If no Energy, r_0 or $\Delta\sigma$ is given, assume that $\Delta\sigma$ = 1 MPa.
3. $\Delta\sigma = 7 * M_0 / (16 * r_0^3)$
4. $\tau_A = E * M_0 / G$
5. $\tau_A = \Delta\sigma$

Table 5-4 Code describing strength of elements on each layer.

Parameter(s)	Notes
NLAYER, NROX, NBED & NTEN	These arrays refer to properties listed in the arrays above.
NROX & NBED	<0 for elastic layer nrox = 0 for zero normal induced stress (free surface) nbed = 0 for zero shear induced stress (free surface) N >= 1 for use of property #N above. N=1 for first value, N=2 for second value, etc.
NROX	Use arrays UCS_* for np = 1 Use arrays UCS_* and FAC_* for np > 1.
NBED	Use arrays C0 and phi
NTEN	Use array T0

6 VCR Seismicity

Milev, A.M. and S.M. Spottiswoode. Effect of the Rock Properties on Mining Induced Seismicity Around the Ventersdorp Contact Reef, Witwatersrand Basin, South Africa, Pure and Applied Geophysics, special issue on induced seismicity, Ed: C Trifu, in Print, 2002.

The final report is **not** available in MS Word format. It is presented here in PDF format as sent from the publishers prior to publication.

7 Aftershocks and foreshocks of mine seismic events.

Presented at 3rd International Workshop on the Application of Geophysics to Rock and Soil Engineering, November 18, 2000, Melbourne, Australia. (prior to GeoEng 2000) by Steve Spottiswoode

7.1 ABSTRACT

Aftershock and foreshock time sequences of blasts and seismic events on four mines were found to follow Omori's law ($n(t) \sim t^{-p}$) with the value of "p" ranging from 0.6 to 1.0. These results were obtained through superposition of the time sequence of many events. On average, less than one additional event took place in the four hours preceding main shocks.

Although aftershocks are not often clearly identified, when superposition is applied they were found to occur at a rate well in excess of the background rate for a few hours. This fact should be considered in seismic risk management and people should be withdrawn over a region around larger events. The recommended times and areas should be decided locally, based on agreed concept of "acceptable" risk and using the methodology described above.

Foreshocks also show the same patterns, particularly for small events when each event was considered as a main shock. Perhaps counter-intuitively, smaller events were preceded by more foreshocks than was the case for larger events. In the data sets studied, there were too few events preceding larger events to be used for short-term predictions. In any case, large events are rarely preceded by an accelerated rate of seismicity.

7.2 INTRODUCTION

Seismicity and rockbursts are an inevitable part of mining in brittle rock at depth. The primary source of seismicity is redistribution of stresses from the mined rock onto the remaining rock mass. Removal of ore and waste typically takes place by blasting. The rate of seismicity is typically very high immediately following the blast and then decays to the background rate after a period of the order of hours.

The rate of earthquake aftershocks decreases approximately inversely with time after large earthquakes, a phenomenon called “Omori’s law”. Utsu et al (1995) presented a thorough review of Omori’s law since the original work by Omori in 1891. Most of their references were to Japanese studies and only two referred to work on mining-induced events, namely McGarr (1976) and McGarr and Green (1978). A dramatic example of aftershocks induced by a controlled mine collapse was provided by Scott Phillips et al (1997). This paper addresses some issues of aftershock behaviour, as caution against the damaging effects of aftershock seems an easy way to control the risk of exposure to rockbursts.

McGarr and Green (1978) found that the rate of tilt and the cumulative rate of aftershocks of large events could be described as logarithmic creep. They also pointed out that this is compatible with Omori’s law which originally postulated that the rate of seismicity, $n(t) \sim 1/(c+t)$, where c is a small constant.

Omori’s law holds a lowly status in geophysics, as physical explanations are not widely accepted. Utsu et al (1995) referred to it as “... one of the few established empirical laws in seismology”. Also: “The power law implies the long-lived nature of activity in contrast to the exponential function appearing in most decay laws in physics”.

Yamashita and Knopoff (1987) have proposed two models in which stress corrosion cracking provides the necessary time dependency. The Gutenberg-Richter Magnitude-frequency distribution of earthquakes, $\text{Log}(n(M)) \sim -bM$, provides a widely accepted power law distributions of seismic source sizes. For a typical value of $b = 1.0$, Yamashita and Knopoff (1987) suggested that the “p” value in Omori’s law should be p=1.

(Malan and Spottiswoode (1997) used simple viscous relaxation laws to generate a logarithmic decay of deformations after the advance of a stope face. The essential element of this work is that the stress relaxation occurs on a range of scales. More recent, unpublished, work by both authors has shown similar results.

7.3 METHODOLOGY

Aftershock sequences are consistently recorded by mine seismic networks in South Africa at present only for the largest events, say M>3. Events with M~= 2 can cause considerable damage and therefore their foreshock and aftershock behaviour is of interest. In this paper, I use the method of superposed sequences (Utsu et al, 1995) for quantifying the average occurrence of both foreshocks and aftershocks.

The matrix (Tij) in Figure 1 represents the time differences between all possible pairs of events "i" and "j" between "N" events. This is illustrated in Equation (7-1).

$$T_{ij} = | t_i^{M} - t_j^{A/F} | \qquad (7\text{-}1)$$

If the "*i*" events are defined as main shocks, then t_j are aftershocks when $t_j > t_i$ and t_j are foreshocks when $t_j < t_i$.

A real-world study of the time-dependent behaviour of foreshock and aftershock behaviour requires more complex analysis than simply analysing the values T_{ij}. For analysis of real data, a time period of complete recording before and/or after any possible main shock is needed. In this paper, one week's data are analysed. Subset of the data for foreshocks and aftershocks are shown in the diagonal bands marked as such. I then exclude main shocks within one week of the start or end of each data set (stippled triangles in Figure 1).

A special exclusion is needed for the normal production blasts for the case of mine events. For the South African gold mines, blasting takes place between about 13:00 and 17:00. For these cases, I only studied main shocks between 22:00 and 10:59 inclusive to minimise the effect of blasting.

In any set of seismic events, any individual event can possibly be construed as leading to later events. Figure 7-1 illustrates application of the method of superposed sequences (Utsu et al, 1995, p 13) to mining events. In the normal case of considering only one or more selected events as the main shocks, data for these events are contained in columns such as that marked in **bold** in Figure 7-1.

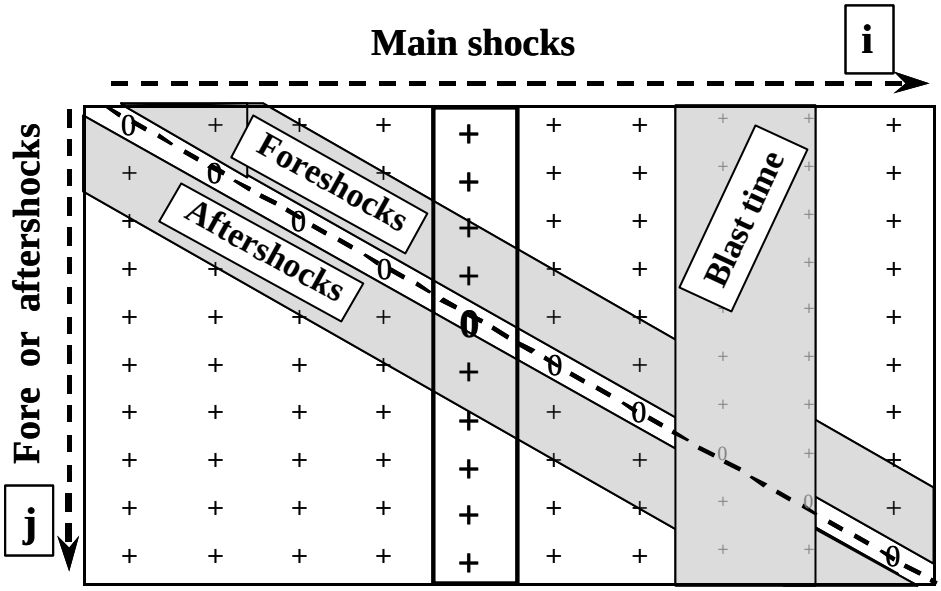

Figure 7-1 A matrix representing all possible foreshocks and aftershocks within a data set. Any column represents a possible sequence of foreshocks, main shocks and aftershocks. One such sequence is in a box and marked with larger symbols. For the full data set, all possible main shocks lie on the diagonal (dashed line and zeroes). Aftershocks and foreshocks within a limited time (one week in this paper) before and after any main shock are shaded. Events in the three lightly stippled areas are excluded for reasons explained in the text.

As in the case of earthquakes, the choice of the size of any aftershock zone requires some subjective judgement. In this report, I simply consider only those events within a defined epicentral distance of each main shock. The vertical distance between events is ignored, as the location error is typically larger in this direction.

Lastly, what happens when each event in the data set is considered as a possible foreshock or aftershock to each event as a possible main shock? As $T_{ij} = T_{ji}$, the distribution of foreshock times is identical to the distribution of aftershock times. Any Omori-type aftershock behaviour is then exactly matched by equivalent foreshock behaviour. The excluded data introduce some exceptions to this behaviour, as will be seen in my analysis.

7.4 DATA

In this paper, I investigate aftershocks of blasts and aftershocks and foreshocks of mining-induced induced events at four mines.

1) Mount Charlotte Kalgoorlie, Australia. (MTC). Mining took place by mass mining of a sub-vertical ore body. Aftershocks following mass blasts of between one and eleven tons of explosives were analysed. Special corrections were necessary to the seismicity rate when blasts were within hours or days of one another.

2) Blyvooruitzicht, Carletonville, South Africa. (BVZ). Pillar removal with preconditioning blasts in which about 100 kg of explosives were blasted 3.5m to 5.5m ahead of advancing faces (Kullmann, 1996).

3) East Rand Proprietary Mines, Boksburg, South Africa. (ERPM) Longwall mining with strike stabilising pillars (McGarr, 1976), McGarr and Green, 1978) and Milev et al, 1995).

4) Tau Tona shaft (WDLE), previously called Western Deep Levels East, Carletonville, South Africa. Longwall mining with strike stabilising pillars.

7.5 ANALYSIS

Aftershock sequences typically follow Omori's law (Utsu et al, 1995, p5):

$$n(t) = K(t+c)^{-p} \qquad (7\text{-}2)$$

where

n(t) = the rate of seismicity,
t = time after the main shock,
K = a constant.
c = a small time offset and
p = a constant

The original work by Omori used p = 1.0, but this was adopted to allow for other values. A value of p ~= 1.0 is usually found.

In Figure 7-2, the seismicity following production blasts at MTC is shown. The log(*n(t)*) vs log(*t*) plot is used as a test of the power-law behaviour implicit in Equation (7-2). The time taken to drop down to the background level is called the "die-down" period and has been used by the mine as guide to the re-entry time into the area after each blast (Mikula, 2000).

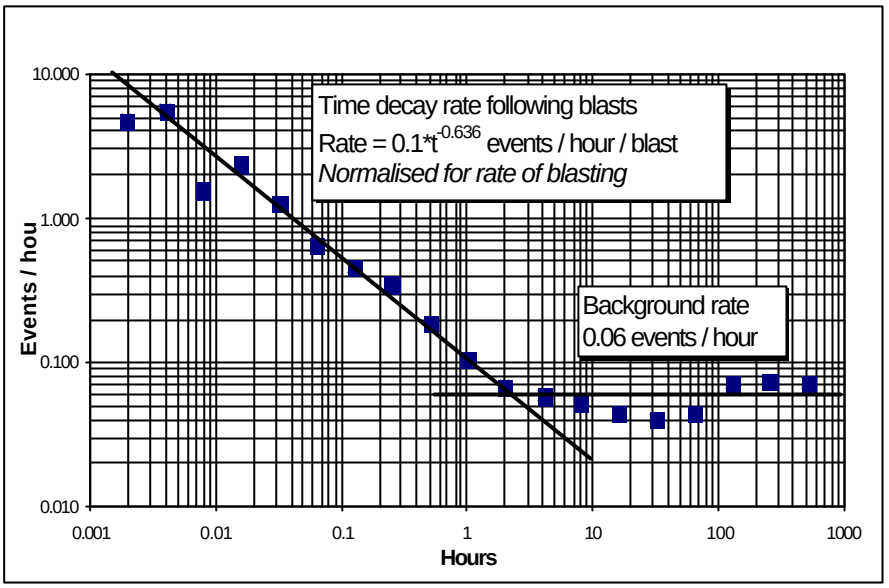

Figure 7-2 Decay of seismicity with time following production blasts at Mount Charlotte Mine (data from Peter Mikula).

Figure 7-3 shows the seismicity rate for events with M>-1.7 at BVZ (Table 7-1). Time bins 5 seconds wide, followed by exponentially increasing bin widths were used. The seismicity rate decayed as t^{-p} until a background seismicity rate of 8 events per day was reached after about one day.

The decay of seismicity after the precondition blast as seen in Figure 7-3 was very well developed because the mining at this site was isolated from other mining and therefore the background rate of seismicity was very low. The increased rate of seismicity following the blasts also indicated that the blast resulted in large changes in the rock mass, as planned.

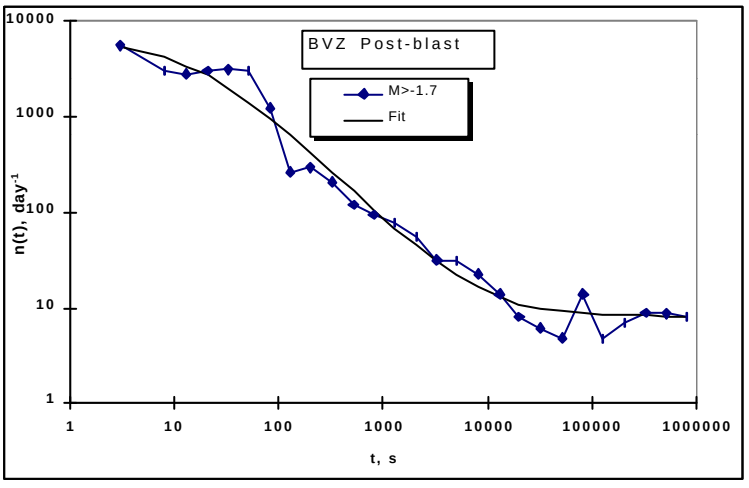

Figure 7-3 Seismicity rate (n(t)) in events per day per precondition blast as a function of time (t) in seconds following 113 precondition blasts, normalised by the number of main shocks. The smooth line is the fit according to Equation (7-3).

As it was difficult in all data sets to separate aftershocks from the background seismicity, Equation (7-1) was adjusted as follows:

$$n(t) = n_{\infty} + K(t+c)t^{-p} \qquad (7\text{-}3)$$

where n_{∞} represents the background rate of seismicity.

Data were then inverted for n_{∞}, *a, K* and *p* to obtain a least-squares fit to the logarithm of *n(t)*. Figure 7-3 shows the application of Equation (7-3) to events with M>-1.7 following 65 precondition blasts. Values of n_{∞}, *a, K* and *p* are listed in Table 7-1.

I then tested the behaviour of larger seismic events outside the blasting windows. Main shocks occurring between 20:00 and 12:00 each day were chosen. Figure 4 shows the decay rates **before and after** seismic events with M>-1.7 and M>1.0. Data for foreshocks and aftershocks were superimposed in Figure 4. The only difference between the plots for foreshocks and aftershocks is caused by the exclusion of events during the blast window. Without this exclusion, these graphs would coincide exactly.

At short times, the aftershocks of M>1.0 events were generally several times more numerous than aftershocks of all the events. On the other hand, the M>1.0 events exhibited very few foreshocks, with the fit to *n(t)* barely rising above the noise level. The irregular curve for the foreshocks of events with M>1.0 in Figure 7-4 was due to the lower number of main shock events (50) and the smaller number of foreshocks. From these data, it seems that there is potentially a better chance of anticipating that small events (M<1.0) are imminent compared to larger events (M>1.0).

The background level following and preceding the larger events was lower than that for the smaller events. One possible explanation is that the larger events occur on structures less intimately associated with the stoping than is the case for the smaller events. It seems that, in general, the smaller events are spatially distinct from the larger events. The most important seismic feature at this site is the up-dip and down-dip edge of the stabilising pillar that was mined (Kullmann, 1995). Larger events tended to follow the pillar, whereas smaller events were associated with the advancing faces.

Table 7-1 List of parameters for foreshocks and aftershock sequences analysed here. "N_{MAIN}" is the number of main shocks. "Distance" is the search radius on plan for identifying foreshocks or aftershocks. B/A/F: "B" for aftershocks of blasts, "A" for aftershocks of mine events and "F" for foreshocks of mine events. N is the average number in excess of the background, measured from the first 4 hours of data.

Mine	N_{MAIN}	Distance	M_{MIN}	M_{MAIN}	B/A/F	$n_{¥}$	*c, s*	*p*	N
MTC		-		Blasts	B	1.44	0	0.64	-
BVZ	113	50	-1.7	Blasts	B	8.1		1.1	6.54
BVZ	3326	50	-1.7	-1.7	A/F	7.2		0.69	0.30
BVZ	47	50	-1.7	1.0	F	3.0		0.66	0.00
BVZ	47	50	-1.7	1.0	A	2.3		0.74	1.98
ERPM	3129	300	0.0	2.0	A/F	0.26	3	0.86	0.06
ERPM	82	300	0.0	2.0	F	0.21	0	1.04	0.04
ERPM	82	300	0.0	2.0	A	0.17	6	1.10	0.19
WDLE	12740	250	0.0	0.0	A/F	10.4	4	0.93	2.24
WDLE	326	250	0.0	2.0	F	4.4	0	0.54	0.24
WDLE	326	250	0.0	2.0	A	4.2	20	0.76	0.59

How many precursory events are involved? Table 7-1 lists the cumulate number of seismic events in the four hours prior to, or following, the main shock, with the background rate of seismicity ($n_{¥}$ in Equation (7-3) above) removed. This supports the contention that smaller events are more "predictable" than larger events.

The value of this precursory pattern for small events is, however, of doubtful value as it is results from symmetry. If all events are considered to be main shocks and stacked at time zero, then the time sequence of foreshocks and after shocks is identical. We have, then, a situation in which aftershock sequences also appear as foreshock sequences. Foreshock sequences also follow Omori's law (Equation (7-2)), but with time (*t*) describing time **before** the main shock.

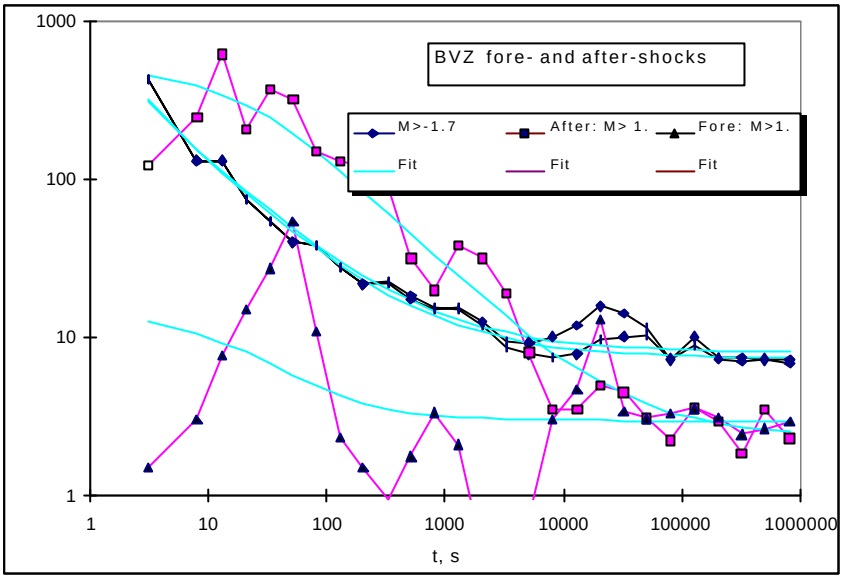

Figure 7-4 Seismicity rate at BVZ in events per day preceding and following events with M>-1.7 and M>0. Symbols as for Figure 7-3.

Figure 7-5 is an analysis of data from ERPM mine (Milev et al, 1995). These graphs are not as well separated as those for data from BVZ. Aftershocks are only slightly more numerous than foreshocks.

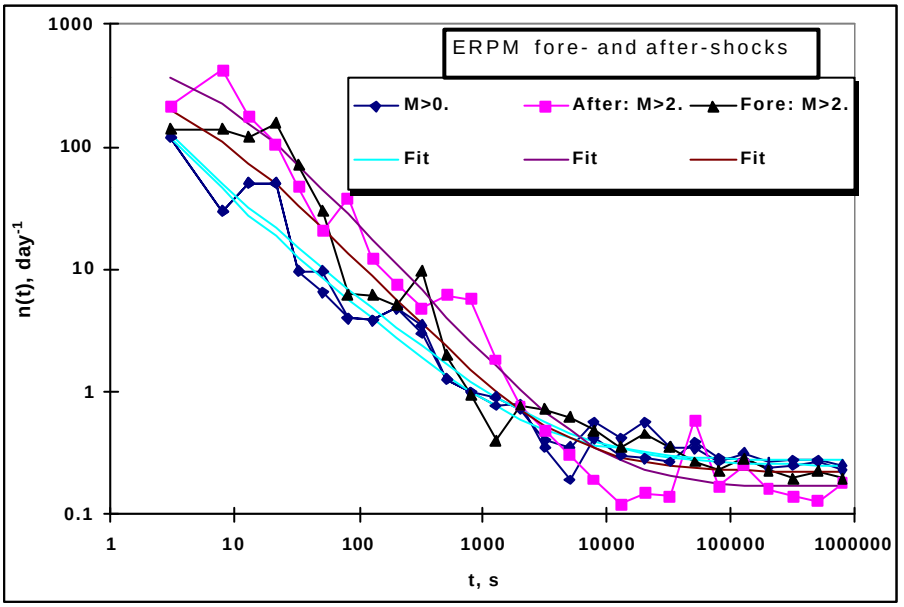

Figure 7-5 Seismicity rate at ERPM in events per day preceding and following events with M>0.0 and M>2.0. Symbols as for Figure 7-3.

Figure 7-6 shows foreshock and aftershock time sequences for WDLE. There is anomalous behaviour at times less than about one minute due, perhaps, by timing problems in the seismic system at the mine. Nonetheless, the general behaviour is similar to that of the data from BVZ.

The large increase in seismicity, typically 100 to 1000-fold in the figures shown here, occurs over only a few seconds to minutes. Table 7-1 lists a number of derived parameters, including the number of events in excess of the background rate of n_∞ between the main shock and four hours before or after the main shock. Only in the case of the precondition blasts did an additional number of more than one event, on average, take place, either before or after the main shocks.

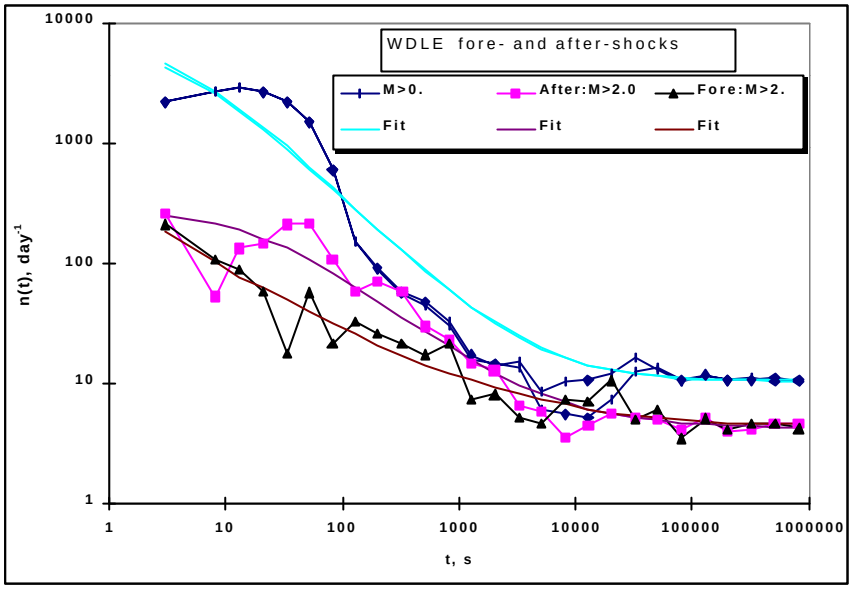

Figure 7-6 Seismicity rate at WDLE in events per day preceding and following events with M>0.0 and M>2.0. Symbols as for Figure 7-3.

7.6 CONCLUSIONS

Aftershock time sequences after blasts and mining induced events were found to follow Omori's law. Foreshocks of induced events also showed the same pattern, particularly for small events. These results were obtained through stacking of the time sequence of many events outside of the blasting time. On average, less than one additional event took place in the four hours preceding main shocks. Smaller events were better "forecast" than larger events.

Although aftershocks are not very common, they occur at a rate well in excess of the background rate for a few hours. This fact should be considered in seismic risk management and people should immediately move to safer area following larger events. The recommended times and areas should be decided locally, based on agreed concept of "acceptable" risk and using the methodology described above.

7.7 ACKNOWLEDGEMENTS

This work was done with support of the Safety in Mines Research Advisory Committee (SIMRAC) under projects GAP608 and GAP722. I would like to thank Francois Malan, Ewan Sellers and van Zyl Brink for comments and suggestions, Michael Nxumalo for finding literature on Omori's law and Peter Mikula for providing the data from Mount Charlotte Mine.

8 Synthetic seismicity mimics observed seismicity.

Keynote address: Synthetic seismicity mimics observed seismicity in deep tabular mines, by Steve Spottiswoode,

presented at the Fifth International Symposium on Rockbursts and Seismicity in Mines, The Dynamic Rockmass Response to Mining

18-20 September 2001 Mount Amanzi Hartbeestpoort

8.1 SYNOPSIS

After decades of only limited interaction between the disciplines of numerical modelling of the behaviour of the rock mass around mines and the recording and analysis of seismicity, we are now faced with the realisation that both disciplines provide an incomplete and limited view on the likely response of the rock to future mining. In the case of modelling, uncertainties about the geological conditions and virgin stress are compounded by questions about the constitutive laws that are supposed to describe rock failure. Further technical and computational difficulties arise from the application of existing constitutive laws. Calibration of any modelling requires careful back-analysis using seismicity and other measures of stress or deformation. The rate of seismicity is generally proportional to the rate of mining, but cannot directly account for any changes in mining geometry or geology. There is a need for each of these disciplines, modelling and seismology, to adapt to one another in order to develop an integrated approach to mine design to control seismicity and rockbursting. This paper attempts to motivate the use and calibration of models that mimic seismicity.

8.2 INTRODUCTION

“What happens when the earth suddenly ruptures? How does it move? What equations describe this? What underlies the variety of earthquake behaviors? Both observations alone and theory alone are too underconstrained to answer these questions by themselves. It is only through an active interplay between observations and theory that we can crack this problem.” (Extract from the web page of Bruce Shaw.)

The need for an “active interplay between observations and theory” is equally important for answering questions about rockbursts and seismicity in mines. Deep-level mines leave large areas of ground as stability pillars and use yielding support systems with the express purpose of controlling rockburst damage. Similarly, various mining methods even at depths less than 1000 m below surface result in rockbursts associated with over-stressed ground and geological complexities (Brummer, 1999). Despite considerable cost and effort to control rockbursts, they continue to be a major threat to the safety and viability of deep-level mining. Durrheim et al (1997) reported on investigations of 21 rockbursts and suggested that: “In the short term the most important lever for reducing the rockburst hazard is the effective implementation of existing rock engineering knowledge and technology”. Two such existing technologies are mine layout design, aided by numerical modelling, and mine seismicity recording and analysis.

The first stated objective of this symposium is: “to promote fundamental and applied research into the dynamics of the response of rock masses to mining induced stress changes”. Why is there a need to promote such research? The most basic explanation is that neither application of numerical modelling nor studies of seismicity have eliminated rockbursts, especially within the constraints of practical mining scenarios. Worse still, we have no reason to believe that mine layout design and sequencing to control rockbursts is close to being optimal. A knowledge base has been built upon each of these technologies and the two knowledge bases are largely independent of one another. It is proposed, therefore, that one of the longer-term “levers” for reducing the rockburst hazard is to develop ways of getting the disciplines of numerical modelling and seismology to work closer together and to “integrate” their work and form a common approach. A number of workers are grappling with various concepts and some are presenting their work at this symposium.

There has been a growing realisation of the need for this integration. In South Africa, for example, two large research projects have recently been completed. Mendecki et al (2001) have investigated the suitability of a number of numerical modelling programs for integration with seismicity. They stated:

“The basic requirements to be met by an integration-ready numerical model of rock-mass response to mining are:

1. It must be designed to solve a forward-in-time problem about the evolution of the physical state of the rock-mass.

2. It must be equipped with the capability of converting the parameters of a real seismic event into a corresponding model-compatible input in the form of an additional loading on the rock-mass.

3. It must allow for an unambiguous identification and quantification of “seismic events” among the model-generated data.”

As part of meeting the challenge of mining at greater depths (Vieira and Durrheim, 2001), Spottiswoode et al (2001) tested two approaches to integration. These approaches are summarised and expanded by Lachenicht et al (2001), Wiles et al (2001) and in the current paper.

Evidence of the wisdom, or prescience, of the symposium objective of promoting integration of modelling and seismicity is the large number of papers submitted that cover this topic. I have been fortunate to see some of these papers and reference will be made within the text to these papers. My paper is structured as follows:

- Aspects of numerical modelling relevant to seismicity.
- Aspects of seismicity relevant to numerical modelling.
- A brief review of previous work aimed at integrating seismicity and modelling.
- A summary of my own efforts at integration of modelling and seismicity.
- Conclusions.

8.3 Aspects of numerical modelling relevant to seismicity.

The most important motivator in the development of modelling of the rock mass in mines was recognition that the rock mass around deep-level mines behaves elastically. Exceptions to elastic behaviour were made for regions in which the stresses exceed the strength of intact rock and where geological weaknesses were mobilised. Cook et al (1966) proposed that the Energy Release Rate (ERR) was a suitable explanation for the occurrence of seismicity associated with advancing faces. This work was supported by a number of studies including McGarr and Wiebols (1977). The relationship between ERR and rockburst incidence received further recognition by the publication of the South African “Industry Guide to Methods of Ameliorating the Hazards of Rockfalls and Rockbursts” (Anon).

To some, it might have seemed that control of seismicity was a simple affair and would be achieved through the use of large regional stability pillars to reduce the volume of elastic convergence and hence the average ERR. However, this stance was softened in the 1999 guide (Jager and Ryder, 1999) when the role of geotechnical conditions was recognised. While identified geotechnical conditions were recognised as playing a role in the amount of seismicity

per area mined, the variations in the amount of seismicity even with similar geotechnical conditions were still large (often more than a factor of three) (Milev and Spottiswoode, 1997).

The long history of development of science and engineering has been characterised by the development of "models" that describe the behaviour of the natural world. Underlying these models are physical laws and established theories. These laws and theories have led to scientific advances that have allowed us to build conceptual models of the physical world around us. The Excess Shear Stress (ESS) concept (Ryder, 1988) is an example of the use of a simple physical law (Coulomb failure) to explain and predict the total amount of shear slip on faults near mine excavations. Unfortunately, construction of explanations for common occurrences is not always easily accomplished in terms of these basic physical laws. Bak (1996) aptly expressed this by entitling a section of his book (page 3): "The Laws of Physics Are Simple, but Nature Is Complex". The work of Bak is well illustrated by models of growing or rolling sand piles in which avalanche sizes follow power-law distributions, similar to the Gutenberg-Richter relationship for earthquakes.

A growing literature of earthquake simulations has shown that generation of seismicity can be made to follow similar patterns (e.g. Shaw and Rice, 2000) using either slip or velocity weakening behaviour in elastodynamic models of planar fault slip. Spottiswoode (1999) found that even simpler "rules" could be used in which instantaneous stress drop on over-stressed rock generates suites of synthetic seismic "events" similar to observed seismicity.

The main objective of this paper is to persuade the reader that the additional effort that is required to mimic the observed seismicity catalogue will be rewarded by better understanding of the drivers of seismicity and finally more rational mine layout design to control seismicity and rockbursting.

8.4 Aspects of seismicity relevant to numerical modelling

The last 20 years has seen an explosion of the size of the data set of digitised seismograms from underground recordings. However, interpretation of mine seismic events is still largely based on the approach developed for earthquakes, with their slip mechanisms being described in terms of simplified source processes. Source mechanism studies, such as those of Trifu and Disley (2001) and Andersen and Spottiswoode (2001) are the exception rather than the rule and the paper by Cichowicz (2001) is a rare attempt to introduce debate into complex source inversions of mine seismic events.

For comparisons with modelling the rock mass around mines, the ideal seismic data would provide accurate distributions of inelastic shear strain in both space and time of all seismic events, as required in point 2 in the Introduction above, from Mendecki at al (2001). Unfortunately, this ideal is not achieved and possibly not achievable and we have data sets that are imperfect in many ways. Let us now consider different aspects of seismicity that are relevant to modelling.

8.4.1 Locations

The location error across many mines, such as the mine-wide networks in the South African mines, is about 50 m in plan. This may be sufficient to identify the nearest working place and to allocate many events to major fault zones, but it is often the case that events locate within complex mining and geological situations, where events cannot be unambiguously allocated to single, well-defined mining (e.g. pillar, face or abutment) or geological structures (e.g. lithological units or discontinuities). New location methods that combine the use of arrival times with arrival-time differences based on picked arrivals and cross-correlations between pairs of events show great promise to "sharpen up" the pattern of locations (Spottiswoode and Milev, 1998 and Waldhauser and Ellsworth, 2000). It is easier to motivate moving the locations to where they might be expected from modelling (2001) once a better three-dimensional picture is obtained of the shape of a source region.

8.4.2 Source dimension.

Estimation of the shape and size of a seismic source region is still most often based on a circular crack with radius provided by the theory of Brune (1970, 1971) and centred at the event hypocentre. Unfortunately, mining provides several factors that are likely to result in major deviation from this simple model:

- Slip on faults such as the San Andreas is limited to about 20 km vertically but may extend laterally for hundres of kilometres (Shaw and Scholz, 2000). Similarly, because most mining involves extraction of ore bodies that are elongated in one or two dimension (pipes or reefs), the largest events will be more limited in their growth away from the workings than pseudo-parallel to the workings.

- The distribution of shear slip will deviate from circular symmetry for events that locate in regions of high stress gradients, for example near working faces.

- “Daylighting” of shear slip into the workings results in extremely asymmetrical slip profiles (Napier, 1991).

The assumption of circular symmetry around the event hypocentre must therefore be questioned, especially for larger events.

8.4.3 Source mechanisms

Problems with obtaining accurate seismic moment tensor solutions are illustrated by Andersen and Spottiswoode (2001) who also introduced an improved methodology using a hybrid of absolute and relative moment tensor inversions.

8.4.4 Time distributions

The rate of seismicity (R(t)) following both blasting and large events is well described by the Omori law (R(t) ~ 1/t), where t is time after a blast or mainshock (2000).

8.5 Previous work on integrating mine seismicity and modelling

McGarr and Wiebols (1977) were the first to show a quantitative relationship between mining and seismicity, as properly quantified in terms of seismic moment. They found that the use of large strike stabilizing pillars reduced the amount of seismicity, measured as the sum of seismic moments, in direct proportion to the reduction in the amount of elastic convergence in a longwall mine where the mining was not controlled by faulting. Ryder (1988) proposed the concept of Excess Shear Stress (ESS) for estimating likely seismicity. Work by Spottiswoode (1988 and 1990) attempted to adapt the concept of ESS to mining on less faulted reefs.

Salamon (1993) extended the ESS concept to slip on a statistical distribution of fault sizes and orientations. Board (1996) applied this method to a known set of structures on a mine and simulated a frequency-magnitude distribution similar to that observed on the mine. The importance of Board’s study was that it quantified the effect of a particular family of structures on the seismicity in a way that could assist in motivating changes in mine design.

Lachenicht and van Aswegen (1999) generated seismic catalogues from explicit slip on a fault peppered by a distribution of asperities with random values of strength.

Two papers by Lachenicht, Wiles and van Aswegen in this Symposium (Lachenicht et al, 2001 and Wiles et al, 2001) make strong claims in favour of imposing inelastic strains, based on recorded seismic events, onto models of on-going mining within otherwise elastic rock and then being able to identify regions of excess stress which are likely sources of future seismicity. As I have suggested in the previous section, the demands on the seismic data that are needed to achieve this might well exceed the capacity of currently available data.

Beck and Brady (2001) summarised previous unpublished work by Beck that combined modelled stress, strength criteria and seismic locations to define the most likely orientation of pre-existing planes of weakness. These planes were found to correlate well with known structural orientations in the mine. In their symposium paper, they describe a procedure whereby, through customised calibration, the stress and stiffness at a three-dimensional mesh of points can be used to estimate likely seismicity during certain extraction sequences.

In summary, the number of papers and also the introduction of new methodologies for integrating mine seismicity and modelling have increased rapidly in the last five years. The field is still so new that it would be premature to presume that any particular method will dominate or even disappear within the next five years.

8.6 Mimicking seismicity

Spottiswoode (1999) showed that simulated seismic catalogues can have generic characteristics similar to observed seismic catalogues. Spottiswoode et al (2001) performed case studies using data from several mines. Firstly, though, a short description of the method of event simulation is needed here. The reader is referred to Spottiswoode (1999) for more details of the Boundary Element numerical code used (MINF).

8.6.1 Simulation method

Once the mining geometries and sequences have been defined and the rock strength specified, the MINF code functions as follows, with reference also to Table 8-1 and Figure 8-1. In the current analysis, simple one-dimensional strength descriptors are applied in which only the normal on-reef stress is considered.

1. Remove rock through stress relaxation on elements that are currently being mined. As element sizes are typically much larger than the face advance per blast (typically 10m and 1m respectively), stresses on the elements to be mined are reduced in stages, say 10 in this case.

2. Test every remaining element for possible seismic failure. Seismic failure is initiated at the point at which the strength of either failed or unfailed rock is exceeded the most and is allowed to grow to any one of its spatial neighbours for which the strength is exceeded until it can spread no further. The event growth is stopped when all neighbours are either too strong or have lost too much strength due to seismic overshoot or viscous post-failure relaxation. During the growth process the normal stress transfer from yielding elements onto all other elements, as provided by the Boundary Element Method, takes place. Repeat this process until no further "seismic" failure is possible, then continue to step 3.

3. Move forward in time a fraction of the time between face advance steps and allow viscous relaxation in proportion to stresses exceeding the final, long-term, strength. Go to step (1) if the next face advance is due; otherwise go to step (2) to test for possible seismic failure.

Table 8-1. Explanation of meaning of rock strength in MINF.

Strength type	Description
Peak	Peak strength of solid rock
Static	Post-failure strength
Dynamic	Seismic overshoot strength
Final	Final, long-term strength

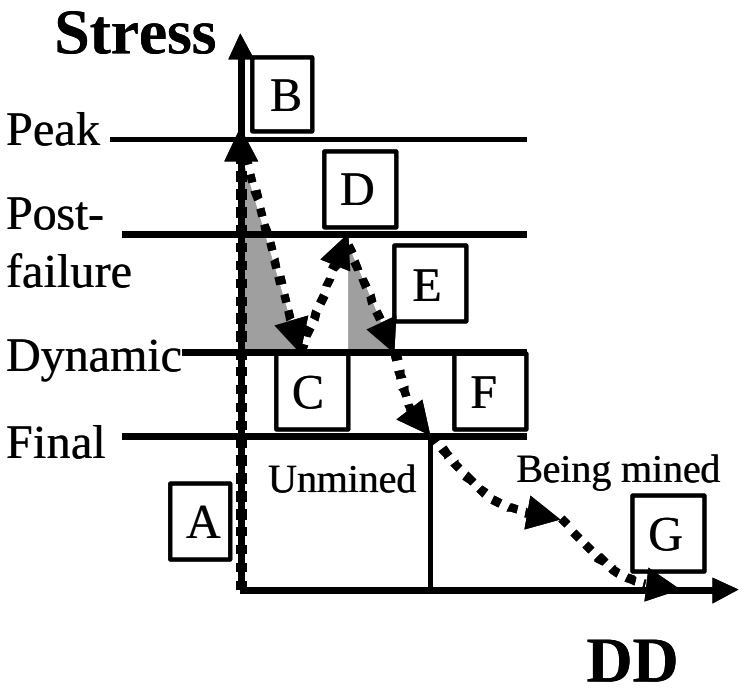

Figure 8-1 Cartoon illustrating a simplified stress-deformation history of an on-reef elementin MINF. Stress increases from virgin stress (A) to the ultimate strength of solid rock (B) as mining advances. Failure occurs and the stress drops along the load line (C), generating a simulated seismic event. Nearby mining or seismicity might increase the stress sufficiently again to initiate another seismic event (D) and the stress drops again along the load line to (E). With time, the stress may drop further to the viscous, long-term, strength (F). Finally, when this element is mined in stages at the face, the stress relaxes viscously with time and instantly with mining step to zero stress (G), with two stages of stress relaxation illustrated here. Lastly, the crosshatched areas are used to characterise the contribution of this element to each of the two events, with the base contributing to the seismic moment and the area to the "radiated" energy.

Each "event" can be described by the same source parameters as those used to describe observed data:

- The location is the point of initiation.
- The time is provided by the representation of the mining history and the time after the most recent face advance, or face "blast".
- The seismic moment is equal to the product of the modulus of rigidity and the "volume" of seismic deformation given by the summed Displacement Discontinuity (DD), as shown in Figure 8-1, multiplied by the area of each element. In the case of the normal stress and DDs, as simulated here, a correction should be made for equivalent inclined shear slip.
- Seismic energy is estimated from the work done on each element in excess of the dynamic strength. It should be noted that negative energy release on individual elements is possible

when slip occurs but the stress after the event is greater than the stress before the event. The overall energy release is, however, always positive.

- In the normal manner, other source parameters such as moment-magnitude and apparent stress are determined from the seismic moment and seismic energy.

8.6.2 Mine simulations

Computer Aided Design (CAD) systems are now widely used on South African gold mines, but are usually deficient in that they cannot easily be used to provide the date at which any section of reef has been mined. This information is required for defining the mining sequence for simulation and then comparison with observed seismicity. Time-consuming manual digitising of paper plans has then been needed. This has had the effect of increasing the time to describe the mining sequence and has severely reduced the amount of mining that has been simulated to date.

In the current work, the method described by Spottiswoode (1999) and also in the previous section of this paper will be applied to analysis of case studies at several mines. Since 1999, I have made a number of enhancements to MINF. The mining was modelled using 64 by 64 or 128 by 128 elements compared to 32 by 32 in Spottiswoode(1999) and the simulations were based on normal on-reef stress only (Spottiswoode et al, 2001). No site descriptions are provided here and the figures are presented to illustrate my main message, namely that simulated seismic catalogues can closely mimic observed seismic catalogues.

The spread of locations (Figure 8-2) is similar, with more scatter evident in the observed seismic locations. The uniformly large symbols and no small symbols for the synthetic seismicity in this case were due to a coarse solution performed on site and therefore a large value of MMIN. The seismicity accompanied the face advance in the lower and right-hand parts of the plots. There was also observed, and simulated, seismicity on the left, associated with old faces that were subject to additional stress by the recent mining.

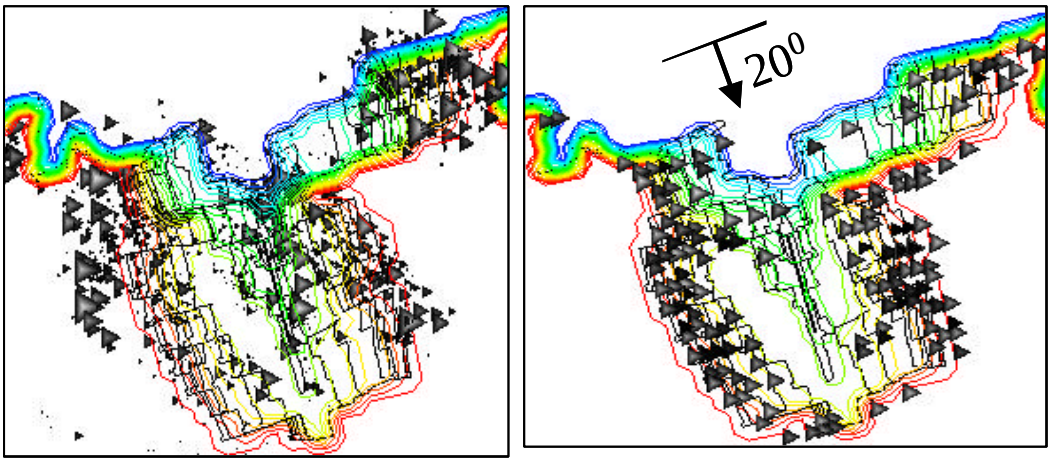

Figure 8-2 History of two years of mining at 3km depth and observed (left) and modelled (right) seismicity associated with this mining. Symbol sizes are proportional to Magnitude.

The **cumulative seismicity**, as measured by cumulative moment in Figure 8-3, has similar "shape" for observed and modelled data. In particular, the observed rate of seismicity, which can be defined as the slope of each curve in Figure 8-3, is well tracked by the model data. In both cases the observed rate of seismicity decreased at about the same time as that predicted by the modelling. This is an extremely practical result as it might allow different mining methods to be simulated in search of some optimum sequence for further mining of problematic areas.

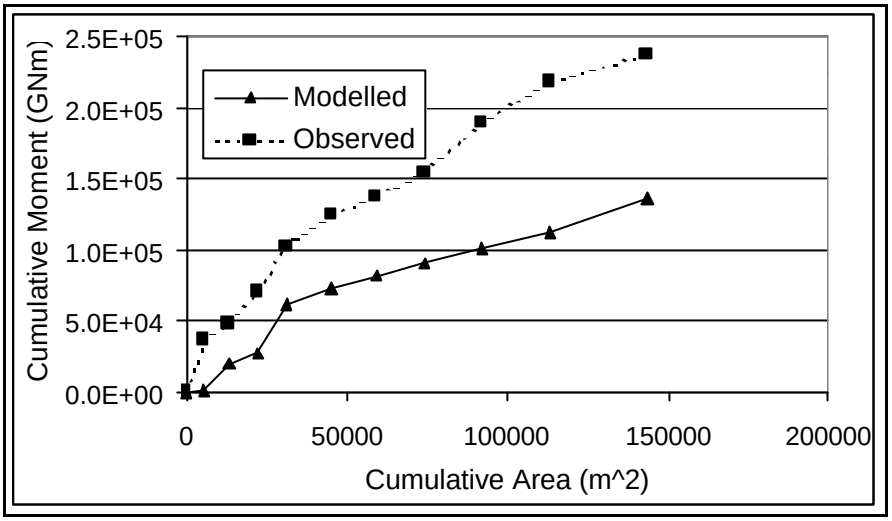

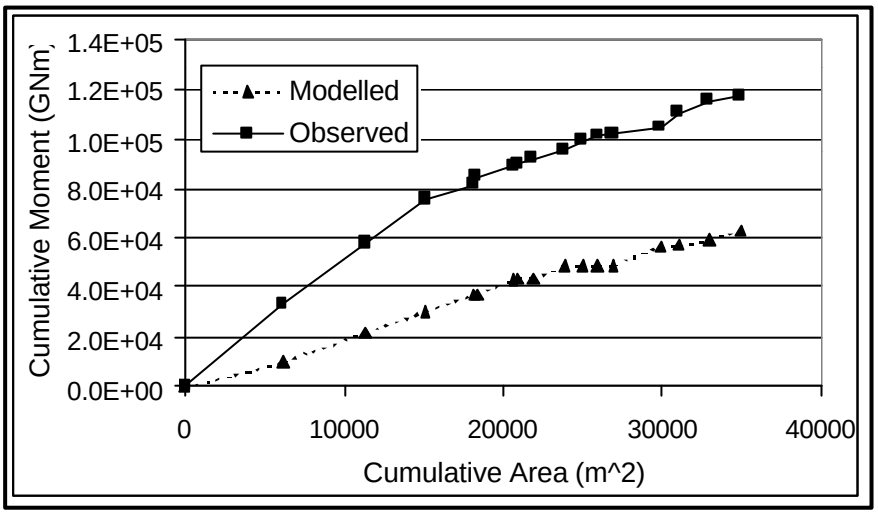

Figure 8-3 Cumulative rate of observed and modelled seismicity as a function of area mined for two mines.

The **frequency-magnitude** relationship is in agreement for events within a range of Magnitudes between 1.0 and 1.5 (Figure 8-4). The minimum magnitude of the modelled data (marked as M_{MIN}) was controlled the element size. The sharp cut-off of the modelled data at M_{MAX} = 2.3 is caused by deficiencies in the model, particularly the two-dimensional distribution of elements. Another cause was that the simulated fracture region typically only advances by one grid size in this type of simulation. The code corrected for generating no events with M>2.5 by generating too many events in the range 1.5 < M < 2.2.

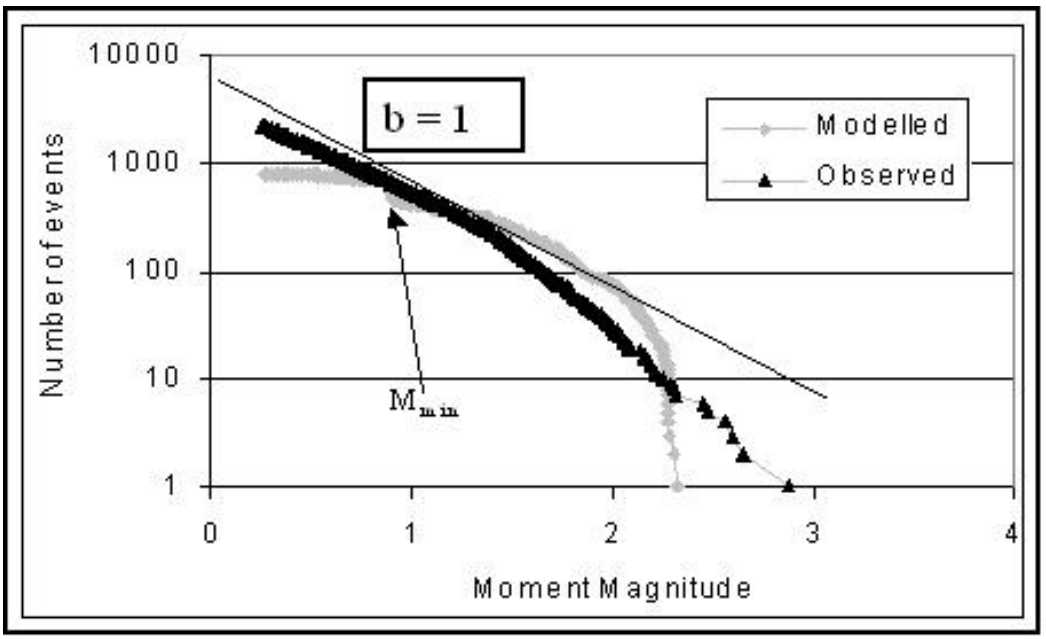

Figure 8-4 Observed and modelled frequency-magnitude distributions, with a reference line with "b" value of 1.0.

The post-blast **distribution of events with time** (Figure 8-5). The seismicity rate followed a logarithmic curve, in broad agreement with logarithmic creep and the Omori's law of aftershocks (Spottiswoode, 2000). The "bumps" in the model curve could have been the result of the small number of events under consideration. Another possible explanation is event clustering in time, perhaps even through aftershocks activity. More detailed investigation is definitely needed into the modelled time dependency.

Insert Figure 5.

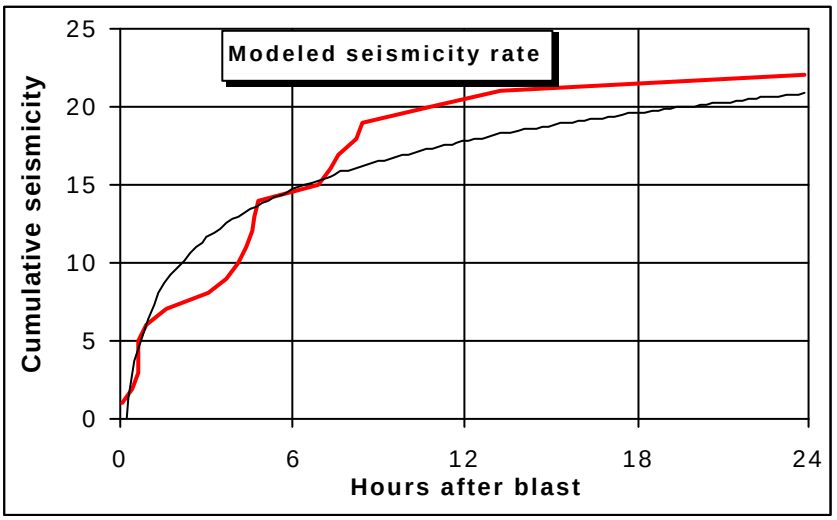

Figure 8-5 Modelled cumulative seismicity with a logarithmic curve for comparison.

8.6.3 Shortcomings of these simulations

Although the correspondence between the observed and modelled seismicity is good as illustrated in Figure 8-2 to Figure 8-5, there are a number of issues, of a fundamental nature, related to the numerical simulations and also to practical applications that must still be addressed. A few of these issues are:

- What controls the slope of the magnitude-frequency distribution? Should it always be b=1.0?

- Is there a physical limit to M_{MAX} that might be encountered in any area and can this limit be provided through modelling?

- Is it possible to overcome problems with grid-size dependence?

- Are quasi-static codes such as MINF even sufficient for simulation of seismicity or are truly dynamic codes needed? This will require comparing simulations done by the two types of code

8.7 Conclusions

As neither the use of numerical modelling nor the study of seismicity on its own is providing a firm basis for mine layout design under rockburst-prone conditions, an increasing number of studies have suggested moving towards an integrated approach using both disciplines. Each discipline must be adapted to find common ground and different methods have been proposed. In this paper, synthetic seismic catalogues have been shown that mimic observed catalogues in several ways, such as spatial distribution, cumulative seismic moment as a function of cumulative area mined, frequency-magnitude distributions and seismicity rate following the blast. The good results using the cumulative seismic moment are particularly encouraging

when considering choices amongst mine planning options. A number of outstanding questions must still be addressed during the course of further work.

8.8 Acknowledgements

Thanks to John Napier, Roger Stewart and Fernando Vieira for reviews of drafts of the manuscript. This paper was supported by SIMRAC project GAP722. The sponsors of the Deepmine Programme are thanked for permission to publish some of the results of the work under Task 5.2.1.

REFERENCES

Aki, K 1965 Maximum Likelihood Estimate of b in the Formula Log N = a - bm and its Confidence Limits, *Bull. Earthquake Res. Inst., Tokyo Univ. 34*, pp237-239.

Andersen, L.M. and Spottiswoode S.M. 2001 A hybrid relative moment tensor methodology. *Rockbursts and Seismicity in Mines – RaSim5*, South African Institute of Mining and Metallurgy, pp 81-90.

Anon. 1988 An Industry Guide to Methods of Ameliorating the Hazards of Rockfalls and Rockbursts, *Chamber of Mines Research Organisation*.

Bak, P. 1996 How nature works: the science of self-organized criticality. *Springer-Verlag*.

Beck, D.A. and B.H.G Brady. 2001 A numerical method for engineering management of induced seismic risk in hard rock mining. *Rockbursts and Seismicity in Mines – RaSim5*, South African Institute of Mining and Metallurgy, pp 457-463.

Board, M. 1996. Numerical examination of mining-induced seismicity, *Eurock '96, Barla (ed.), Balkema,*, pp 1469-1486.

Brummer, R.K. 1999. Simple truths about rockbursts. *Proc. 2nd Southern African Rock Engineering Symposium, Ed. TO Hagan, ISRM Regional Symposium*, pp155-159.

Brune, J.N. 1970. Tectonic stress and the spectra of seismic shear waves from earthquakes, *J. Geophys. Res., vol. 75*, 1970, pp 4997 – 5009. (Correction, 1971. *J. Geophys. Res., vol. 76*, p 5002).

Burridge, R. and Knopoff, L. 1967. Model and theoretical seismicity, *Bull. Seismol. Soc. Am., 57*, p341.

Cichowicz, A 2001. Quantification of complex sources. *Rockbursts and Seismicity in Mines – RaSim5*, South African Institute of Mining and Metallurgy, pp 91-98.

Cook, N.G.W. 1963. The seismic location of rockbursts, *Proceedings of the Fifth Rock Mechanics Symposium, Pergamon Press, Oxford*, p493.

Cook, N.G.W, Hoek, E., Pretorius, J.P.G, Ortlepp, W.D. and Salamon, M.D.G. 1966. Rock Mechanics applied to rockbursts. *J. S. Afr. Inst. Min. Metall.,* pp 435-714.

Durrheim, R.J., Roberts, M.K.C., Haile, A.T., Hagan, T.O., Jager, A.J., Handley, M.F. and Spottiswoode, S.M. 1997. Factors influencing the severity of rockburst damage in South

African gold mines. *Proc. 1st Southern African Rock Engineering Symposium, Ed. RG Gurtunca and TO Hagan, SANGORM*, pp17-24.

Esterhuizen, G.S. 1997. An improved method for the assessment of deep mine layouts using elastic models. *Proc. 1st Southern African Rock Engineering Symposium, Ed. RG Gurtunca and TO Hagan, SANGORM*, pp197-204.

Gay, N.C., D. Spencer, D., J.J. van Wyk and P.K. van der Heever. 1994. The control of geological and mining parameters on seismicity in the Klerksdorp gold mining district. *Proceedings Symposium on Rockbursts and Seismicity in mines, Johannesburg, The South African Institute of Mining and Metallurgy*, pp107-120.

Hanks, T.C. and Kanamori, H. 1979, A Moment Magnitude Scale, *J. Geophys. Res. 84*, 2348-2350.

Hofmann, G., Sewjee and van Aswegen, G. 2001. First steps in the integration of numerical modelling and seismic monitoring. . *Proc. 2nd Southern African Rock Engineering Symposium, Ed. TO Hagan, ISRM Regional Symposium.* Pp397-404.

Jager, A.J. and Ryder J.A 1999. A Handbook on Rock Engineering Practice for tabular hardrock mines. *SIMRAC, Johannesburg*.

Kullmann, D.H., Stewart, R.D. and Grodner M. 1996. A pillar preconditioning experiment on a deep-level South African gold mine. *2nd North American Rock Mechanics Symposium, Montreal, Canada,* 375-380.

Lachenicht, R. and van Aswegen, G. 1999. An engineering approach to evaluate the seismic potential of geological structures as a function of mine layout. *Proc. 2nd Southern African Rock Engineering Symposium, Ed. TO Hagan, ISRM Regional Symposium.* pp233-237.

Lachenicht, R. Wiles, T. and G. van Aswegen, G. 2001. Integration of deterministic modelling with seismic monitoring for the assessment of the rockmass response to mining: Part II Applications. *Rockbursts and Seismicity in Mines – RaSim5*, South African Institute of Mining and Metallurgy, pp 389-396.

Lyakhovsky, V., Illchev, A. and Agnon, A 2001 Modelling of damage and instabilities in rock mass by means of a non-linear rheological model. *5th Intl Symposium on Rockbursts and Seismicity in mines, S. A. Inst. Min. Metall*., pp413-420.

Malan., D.F. and Spottiswoode, S.M. 1997. Time-dependent fracture zone behaviour and seismicity surrounding deep level stoping operations, *4th Intl Symposium on Rockbursts and Seismicity in mines, Balkema*, pp173-178.

Malan, D.F. 2002. Simulating the time-dependent behaviour of excavations in hard rock, *To be published in the Rock Mechanics and Rock Engineering Journal*. Report no: 2002-0130.

McGarr, A., Spottiswoode, S.M. and Gay, N.C. 1975. Relationship of Mines Tremors to Induced Stress and to Rock Properties in the Focal Region, *Bull. Seismol. Soc. Am*. 65, 981-993.

McGarr, A 1976 Dependence of magnitude statistics on strain rate, *Bull. Seismol. Soc. Am*., **66,** 33-44.

McGarr, A. 1976. Seismic Moment and Volume Changes, *J. Geophys. Res. 81*, 1487-1494.

McGarr, A. and Wiebols, G.A 1977. Influence of Mine Geometry and closure volume on Seismicity in deep level mine. *Int. J. Rock Mech. Min. Sci., & Geomech. Abstr.,* vol. 14, pp 139-145.

McGarr, A. and Green, R.W.E. 1978. Microtremor sequences and tilting in a deep mine. *Bull. Seismol. Soc. Am*., **68, 6**, 1679-1697.

McGarr, A. 1986, Some Comments on the Nature of Witwatersrand Mine Tremors, *Unpublished report.*

Mendecki, A.J., Napier, J.A.L., Ilchev, A. and Sellers, E. 2001. Fundamental aspects of the integration of seismic monitoring with numerical modelling. *Final Project Report SIMRAC GAP603*.

Mikula, P. 1998 Pers. Comm.

Milev, A. M. and Spottiswoode, S.M. Integrated seismicity around deep-level stopes in South Africa. *Int. J. Rock Mech. & Min. Sci. Vol. 34:3-4*, Paper No. 199, 1997.

Milev, A. M. and Spottiswoode, S.M. 2002 Effect of the Rock Properties on Mining Induced Seismicity Around the Ventersdorp Contact Reef, Witwatersrand Basin, South Africa, Pure and Applied Geophysics, special issue on induced seismicity, Ed: C Trifu, in Print.

Milev, A.M., Spottiswoode, S.M. and Noble, K.R. 1995. Mine-induced Seismicity at East Rand Proprietary Mines, *Technical Note, Int. J. Rock Mech. Min. Sci. & Geomech. Abstr*., **32, 6**, 629-632.

Morone, C. 1998. The effect of loading rate on static friction and the rate of fault healing during the earthquake cycle, *Nature, Vol 391*, Jan., pp 69-72.

Napier, J.A.L. 1991. Energy changes *in a rock mass containing multiple discontinuities. J. S. Afr. Inst. Min. Metall. Vol. 91,* pp 145-157.

Napier, J.A.L. and Malan, D.F. 1997. A viscoplastic discontinuum model of time-dependent fracture and seismicity effects in brittle rock*. Int. J. Rock Mech. Min. Sci. & Geomech. Abstr, vol. 34,* pp. 1075-1089.

Napier, J.A.L. 1998. Three-dimensional modelling of seismicity in deep level mines. *3rd conference on Mechanics of Jointed and faulted Rock. MJFR-3*, Balkema. pp285-290.

Nxumalo, M. 2001 Integration of seismic observations and numerical modelling using elastic modelling at four gold mines. MSc dissertation submitted to the University of the Witwatersrand.

Ortlepp, W.D. 1978 The mechanism of a rockburst. *Proceedings 19th U.S. Symposium on Rock Mechanics, Kim, Y.S. (ed.). Reno, University of Nevada*, p476.

Peirce, A.P., Spottiswoode, S.M. and Napier, J.A.L. 1992. The spectral boundary element method: a new window on boundary elements in Rock Mechanics., *Int J Rock Mech Min Sci & Geomech Abstr, vol 29, No. 4*, pp 379-400.

Roberts, M.K. and Schweitzer, J.K. 1999, Geotechnical Areas Associated with the Ventersdorp Contact Reef, Witwatersrand Basin, South Africa, *J. of S. Afr. Inst. Min. and Metall*. 157-166.

Ryder, J.A. and Napier, J.A.L. 1985. Error analysis and design of large-scale tabular mining stress analyser. In *Proc. of the 5th Int. Conf. on Numerical Methods in Geomechanics Nagoia, Japan*, pp1549-1555.

Ryder, J.A 1988. Excess shear stress in the assessment of geologically hazardous situations. *J. S. Afr. Inst. Min. Metall*, *88*, pp. 27-39.

Salamon, M.D.G. 1984. Energy Considerations in Rock Mechanics: Fundamental Results, *J. S. Afr. Inst. Min. Metall. 84*, 233-246.

Salamon, M.D.G. 1993. Keynote address: Some applications of geomechanical modelling in rockburst and related research. *3rd Intl Symposium on Rockbursts and Seismicity in mines, Balkema*, pp297-309.

Shaw, B.E. and Rice, J.R. 2000. Existence of continuum complexity in the elastodynamics of repeated fault ruptures, *J. Geophys. Res.*.

Shaw, B.E. and Scholz, C.H. 2000. Slip-length scaling in large earthquakes: Observations and theory and implications for earthquake physics, submitted.

Scott Phillips, W., Craig Pearson, D., Edwards, C.L. and Stump, Brian W. 1997. Microseismicity induced by a controlled, mine collapse at white pine, Michigan, *Int. J. Rock Mech. & Min. Sci.* **34:3–4**, Paper No. 246.

Shaw, B.E. and Rice, J.R. 2000. Existence of continuum complexity in the elastodynamics of repeated fault ruptures, *Journal of Geophysical Research, 105*, p23791.

South Africa Geological Survey (1986-1994), Seismological Bulletins, Pretoria, South Africa.

Spottiswoode, S.M. 1988. Total seismicity, and the application of ESS analysis to mine layouts. *J. S. Afr. Inst. Min. Metall. 1988, vol. 88*, pp 109-116.

Spottiswoode, S.M. 1990. Volume Excess Shear Stress and cumulative seismic moments. *Rockbursts and Seismicity in Mines, Charles Fairhurst (ed.), Balkema*, Rotterdam : 39-43.

Spottiswoode, S.M. 1990. Towards 3-dimensional modeling of rock deformation around deep-level gold mines. *Mechanics of Jointed and Faulted Rock, Rossmanith (ed.), Balkema, Rotterdam*: 1133-1146.

Spottiswoode, S.M. 1997. Energy Release rate with limits to on-reef stress. *Proc. 1st Southern African Rock Engineering Symposium, Ed. RG Gurtunca and TO Hagan, SANGORM*, pp252-258.

Spottiswoode, S.M. and Milev, A. M. 1998. The use of waveform similarity to define planes of mining-induced seismic events. *Tectonophysics, vol. 289*, pp. 51-60.

Spottiswoode S.M. 1999. Modelling seismicity and creep on multiple stope-parallel layers. *Proc. 2nd Southern African Rock Engineering Symposium, Ed. TO Hagan, ISRM Regional Symposium*, pp155-159.

Spottiswoode, S.M. 2000. Aftershocks and foreshocks of mine seismic events. *3rd international workshop on the application of geophysics to rock and soil engineering, GeoEng2000, Melbourne Australia*.

Spottiswoode, S.M., Napier, J.A.L., Milev, A.M. and Vieira, F.M.C.C. 2000. The relationship between ERR and seismic energy release for different geotechnical areas, *SIMRAC final project report GAP612c*.

Spottiswoode, S., Nxumalo, M., Andersen, L., van Aswegen, G., Hofmann, G., Sewjee, R. and Lachenicht, R 2002 Integration of Seismic Monitoring and Numerical Modelling, *Final report 5.2.1 for Deepmine*.

Spottiswoode, S.M. 2001. Keynote address: Synthetic seismicity mimics observed seismicity in deep tabular mines. *5th Intl Symposium on Rockbursts and Seismicity in mines, S. A. Inst. Min. Metall*., pp371-378

Trifu, C-I and Disley, N. 2001. Evaluation of failure mechanisms at Kidd Creek Mine, Ontario, from seismic moment tensor inversions. *Unpublished report*.

Utsu, T., Ogata, Y. and Matsu'ura, R. 1995. The centenary of the Omori formula for a decay law of aftershock activity. *J. Phys. Earth*, **43**, 1-33.

Vieira, F., Selfe, D., Dede, T., Maccelari, M., York, G., Spottiswoode, S., Esterhuizen, G., Milev, A., Johnson, R., Webber, S., Arnold, D., Handley, M., Berlenbach, A., Silva, A., Ruskovich, A. and Vlietstra, D. 1998. *Deep Mine Layout Design Criteria: GAP223*, 1335 pp.

Vieira, F.M.C.C and Durrheim, R.J. 2001. Probabilistic mine design methods to reduce rockburst risk. *Rockbursts and Seismicity in Mines – RaSim5*, *South African Institute of Mining and Metallurgy,* pp 251-262.

Waldhauser, F. and Ellsworth, E.L. 2000. A double-difference earthquake location algorithm: method and application to the Northern Hayward fault, California, *Bull. Seismol. Soc. Am.* pp 1353-1368.

Wiles, T., Lachenicht, R. and van Aswegen, G. 2001. Integration of deterministic modelling with seismic monitoring for the assessment of the rockmass response to mining: Part I Theory. *Rockbursts and Seismicity in Mines – RaSim5*, *South African Institute of Mining and Metallurgy*, pp 379-388.

Yamashita, T. and Knopoff, L. 1987. Models of aftershock occurrence. *Geophys. J. R. astr. Soc.*, **91**, 13-26.